UNIVERSITY OF TARTU

Faculty of Science and Technology

Institute of Molecular and Cell Biology

Developmental Biology Chair

Live Imaging of *Drosophila melanogaster* Eye-Antennal Imaginal Disc *Ex vivo* Culture: Craniofacial Morphogenesis

Bachelor's Thesis

12 ECTS

Robin Sarv

Supervisor(s):

Professor Osamu Shimmi, PhD

Vi Ngan Tran, MSc

Tartu 2024

Live Imaging of *Drosophila melanogaster* Eye-Antennal Imaginal Disc *Ex vivo* Culture: Craniofacial Morphogenesis

The *ex vivo* culture and live imaging of *Drosophila* larval eye-antennal imaginal discs provide unique insights into the intricate mechanisms of head morphogenesis. We present a refined *ex vivo* culturing technique optimized for prolonged imaging sessions, during which we defined distinct developmental stages marked by dynamic morphogenetic events, disc fusion, and head cuticle formation. Our investigation reveals the critical role of peripodial epithelium (PE) substructures in mediating fusion events, highlighting their diverse morphological features and functional significance. Additionally, results show that apoptosis, coordinated movement, and fusion of epithelial cells in the imaginal discs are key factors in the morphogenesis of the fly's head region and the formation of head structures.

Key words: Head morphogenesis, *Drosophila*, eye-antennal imaginal discs, fusion, peripodial epithelium (PE)

CERCS: B350 Development biology, growth (animal), ontogeny, embryology

Äädikakärbse (*Drosophila melanogaster*) silma-tundla imaginaaldiskide *ex vivo* eluskoe reaalajas biokuvamine: kraniofatsiaalne morfogenees

Äädikakärbse (*Drosophila melanogaster*) vastse pea-näopiirkonna struktuuride kujunemine ja morfogenees on seotud silma-tundla algete – imaginaaldiskide – arenguga. Antud bakalaureusetöö eesmärgiks seati välja töötada täiustatud *ex vivo* metoodika dünaamiliste, pikemaaegsete arenguprotsesside reaalajas biokuvamiseks, mille abil välja selgitada, kuidas ja milliste protsesside abil silma-tundla imaginaaldiskid osalevad äädikakärbse vastse peapiirkonna struktuuride kujunemisel. Bakalaureusetöös saadud tulemused näitasid, et silma-tundla imaginaaldiskide päritolu epiteliaalsete rakkude apoptoos, koordineeritud liikumine ja liitumine on võtmetegurid äädikakärbse peapiirkonna morfogeneesis ja struktuuride formeerumisel.

Märksõnad: Pea morfogenees, imaginaaldisk, liitumine, peripodiaalne epiteel (PE)

CERCS: B350 Arengubioloogia, loomade kasv, ontogenees, embrüoloogia

TABLE OF CONTENTS

TABLE OF CONTENTS 3
GLOSSARY OF TERMS, ABBREVIATIONS AND ACRONYMS 5
INTRODUCTION 6
1. LITERATURE REVIEW 7
1.1. EPITHELIAL STRUCTURE 7
1.1.1. Morphology of Epithelial Cells and Epithelia 7
1.1.2. Epithelial Morphogenesis 8
1.1.3. Control of Cell Shape During Epithelial Morphogenesis 9
1.1.4. Fusion of Epithelia 11
1.2. *DROSOPHILA* HEAD MORPHOGENESIS 12
1.2.1. Eye-Antennal Imaginal Discs, Larval Precursor of Head Structure 12
1.2.2. The Missing Gap of Imaging Head Development in Drosophila 15
1.2.3. Adult Head Structures 16
1.3 *DROSOPHILA* HEAD AS AN IDEAL MODEL FOR 3D MORPHOGENESIS 17
1.3.1 Advantages of Using Drosophila as a Morphogenesis Model 17
1.3.2. Genetic and Molecular Tools Employed in Drosophila 18
1.3.3. Ex vivo Approaches in Drosophila 20
1.4. Introducing Head Morphogenesis as a Model System 21
2. EXPERIMENTAL PART 23
2.1. AIMS OF THE THESIS 23
2.2. MATERIALS AND METHODS 23
2.2.1. Fly Stocks and Genetics 23
2.2.2. Culture Media Compositions 25
2.2.3. Dissection and Imaging 26
2.2.4. Microscopy 27
2.2.5. Central PE cell area analysis 27
2.3. RESULTS 29
2.3.1. Long Term Ex vivo Culture and Live Imaging of Drosophila Larval Eye-Antennal Imaginal Discs 29
2.3.1.1. A Method to Image Imaginal Disc Development *Ex vivo* 29
2.3.1.2. Observing Developmental Stages from 2D to 3D during *Ex vivo* Live Imaging 31
2.3.1.3. *Ex vivo* and *In Vivo* Comparison 35
2.3.2. Peripodial Epithelium Dynamics During the Fusion Ex vivo of The Eye-Antennal Imaginal Discs 36
2.3.2.1. PE Structures Involved in Fusion During Head Morphogenesis 36
2.3.2.2. Mechanisms and Location of Fusion in Eye-Antennal Imaginal Discs 41
2.3.3. Levels of Patterned Apoptosis are Elevated in a Band of PE Cells During Morphogenesis 43
2.4. DISCUSSION 47
CONCLUSION 51
RESÜMEE 52
REFERENCES 54

NON-EXCLUSIVE LICENCE TO REPRODUCE THE THESIS AND MAKE THE THESIS PUBLIC 62

GLOSSARY OF TERMS, ABBREVIATIONS AND ACRONYMS

APF – After Pupation Formation

DIC – Differential Interference Contrast

DP – Disc Proper

ECM – Extracellular Matrix

EMT – Epithelial–Mesenchymal Transition

FLP – Recombinase Flippase

FRT – Flippase Recognition Target

FRT cassette – Genetic Information between FRTs

Gal4 – Yeast transcriptional Activator in GAL4/UAS System

GAL80ts – Yeast Temperature Sensitive GAL4 Repressor

GFP – Green Fluorescent Protein

L1 – First Instar Larva

L3 – Third Instar Larva

M – Marginal Zone

MET – Mesenchymal–Epithelial Transition

PE – Peripodial Epithelium

RFP – Red Fluorescent Protein

RNAi – RNA Interference

UAS – Upstream Activation Sequence in GAL4/UAS System

INTRODUCTION

Head morphogenesis is a key developmental process that requires a series of molecular and morphogenetic events. In the fruit fly *Drosophila melanogaster* (referred to as *Drosophila* throughout the thesis), this process involves the fusion of a pair of eye-antennal imaginal discs, which undergo complex cellular changes to form the head and its appendages. However, the morphogenetic events and mechanisms that drive this process are not yet fully understood, mainly due to the difficulty of visualizing the eye-antennal imaginal discs *in vivo* during metamorphosis, when the 2D eye-antennal discs transform into a 3D structure.

This is why this project aims to develop an improved and unique *ex vivo* culture method to track head morphogenesis in real-time. Additionally, by employing this method, the project seeks to achieve a detailed, step-by-step understanding of the transition from third instar larval eye-antennal imaginal discs to the pupal head eversion stage, while also exploring the molecular mechanisms necessary for progressing to subsequent developmental stages.

In this study, we developed an *ex vivo* culture method that allows us to observe the head morphogenesis process in real-time using 5D imaging (XYZ dimensions, time, and wavelength), enabling us to construct 3D videos of the developmental process. Our observations reveal for the first time the process by which a pair of eye-antennal imaginal discs can invert, migrate, and dynamically fuse to form a symmetrical head that includes compound eyes, ocelli, antennae, and head epidermis. During head formation, the peripodial epithelium plays a more pivotal role than previously thought, as it facilitates the fusion of separate discs. By exploring the molecular mechanisms, we found that caspase activity in the edge cells is required for the migration and fusion of the epithelial cells. This caspase activity coordinates growth and cell behaviour in eye-antennal imaginal discs, ultimately leading to the formation of a symmetrical head. In conclusion, apoptosis, coordinated movement, and fusion of epithelial cells in the imaginal discs are key factors in the morphogenesis of the fly's head region and the formation of head structures.

1. LITERATURE REVIEW

1.1. Epithelial structure

1.1.1. Morphology of Epithelial Cells and Epithelia

The epithelium is one of the most common forms of tissue organization in the animal body. It forms cohesive sheets of interconnected adherent cells, creating boundaries between the body's compartments and enveloping organ surfaces. One of the fundamental features of each epithelial cell is polarity, with primary domains including the apical domain facing the sheet's surface, and a basolateral domain facing the underlying tissue and engaging with the basal lamina. The basal lamina separates the body's interstitial space from the basolateral domain as a barrier between connective tissue and the epithelium. (Ganz, 2002; Tepass et al., 2001).

Cell polarity is maintained through the cellularly localized asymmetric distribution of distinct proteins, lipids, and organelles along the apical-basal axis (Schneeberger et al., 2018). Specialized protein complexes, including Par, Crumbs, and Scribble, maintain this spatial segregation. The Par complex regulates apical domain specification and polarity maintenance (Aranda et al., 2008). Crumbs complex is essential for apical membrane identity and junctional integrity (Bulgakova & Knust, 2009). Scribble complex is critical in basolateral domain specification and epithelial polarity (Piroli et al., 2019).

In a mature epithelial cell, cell-cell junctions form around the border of the apical domain. These junctions include the adherens junctions, connecting neighbouring cells, and the tight or septate junctions that seal cell-cell contacts. These junctions interact with apical actin, which, in turn, interacts with lateral and basal actins. The basal actins bind to integrins engaged with the basal lamina, collectively regulating the actin cytoskeleton. Therefore, changes in the actin cytoskeleton in one area can influence other areas. Similarly, intracellular trafficking pathways direct specific cargo to the apical or basolateral domains, thereby controlling polarity through cargo distribution (Tepass et al., 2001). Epithelial structure may appear static, but establishing, remodelling, and maintaining epithelial cells requires continual dynamic interactions between adherens junctions, cytoskeletal proteins, polarity cues and intercellular trafficking (Baum & Georgiou, 2011).

Epithelial cells display remarkable diversity in structure and organization, reflecting their roles in maintaining tissue homeostasis and supporting specialized functions. Understanding tissue function involves recognizing the different types of epithelia that form the tissue. Epithelial cells are organized based on their shape and the number of layers they comprise. Simple

epithelia consist of a single layer, whereas stratified epithelia contain two or more layers. Pseudostratified epithelia consist of a single layer of cells with varying sizes, giving the appearance of being stratified or layered. Epithelia are comprised of three primary cell morphologies: squamous, cuboidal, and columnar. Squamous cells, characterized by their flattened, scale-like morphology, form thin, permeable barriers. They facilitate diffusion, filtration, and provide mechanical stress and protection against pathogens (Scherzad et al., 2019). Cuboidal cells, cube-shaped with a centrally located nucleus, exhibit uniform dimensions with equal height and width. They are involved in secretion, absorption, and molecular transport across the epithelial barrier, playing vital roles in maintaining tissue integrity. Columnar cells, taller than they are wide, have a rectangular, column-like shape, with elongated nuclei typically near the basal membrane. These cells may feature microvilli or cilia and contribute to absorptive or secretory functions (Jia et al., 2022). There are also transitional epithelial cells, specialized for stretching and distension, allowing tissues to accommodate changes in volume. They exhibit variable shapes, ranging from cuboidal to squamous, depending on tissue distension (Kurn & Daly, 2024; W. Yu & Hill, 2011).

1.1.2. Epithelial Morphogenesis

The formation of complex tissue structures is a critical aspect of development, involving epithelial morphogenesis, a complex process that transforms a two-dimensional sheet of cells into a three-dimensional structure. This process can be compared to origami, where paper is folded to create a three-dimensional object (Zartman & Shvartsman, 2010). This transformation entails intricate steps such as morphogen establishment, which leads to spatial information gradients across the tissue, interpreted by cells to differentiate into distinct types with characteristic gene-expression profiles. Unlike origami, epithelial morphogenesis incorporates additional complexities like cell division, apoptosis, and cell-neighbour exchange. Furthermore, within a single epithelial sheet, successive rounds of patterning and morphogenesis are intricately linked, as the outcome of each round influences the initial conditions for the subsequent movements, thus forming a continuous morphogenetic progression (Mendonca et al., 2021; Osterfield et al., 2017).

The fundamental question in developmental biology is how one can pattern an epithelial sheet to achieve a specific desired shape in order to form organs and structures for the developing organism. However, answering this question is challenging due to various factors. These factors collectively alter patterning through mechanical forces generated during morphogenesis, which

initiate at the microscale level with highly localized deformations that accumulate into macroscale folding events, such as invagination and folding. When delving deeper into the cellular level, it turns out that the final outcome depends heavily on factors such as cell shape changes, neighbour exchanges, cell intercalation, as well as cell death, delamination, and cell division. Particularly, cell shape changes and cell intercalation have proven themselves to be key, and sometimes the sole, contributors to tissue reorganization. While forming simple structures from an epithelial sheet may seem intuitively simple, attempting to form complex organs and structures requires more information than we currently possess. Therefore, it remains one of the major questions in the study of developing organisms (Gillard & Röper, 2020; Sakar & Baker, 2018).

1.1.3. Control of Cell Shape During Epithelial Morphogenesis

One of the most common events associated with epithelial morphogenesis is the reorganization of cell shape. Cell shape changes refer to modification in the dimension of one or more sides of cells within an epithelial sheet. These changes depend on the localized reorganization of the cytoskeleton and are often mediated by actomyosin contractile forces and adhesion molecules. In all cell shape changes, alterations in tissue shape induce adjustments in cell packing and shape, and vice versa. Thus, changes in cell shape and tissue structure are intricately connected, serving as two ends of the same stick in morphogenesis (Girdler & Röper, 2014; Schöck & Perrimon, 2002).

At the core of the cell shape change process lies the critical role of cell adhesion, where the intricate interplay between cells and the extracellular matrix (ECM) governs tissue dynamics, directing cellular behaviours crucial for morphogenesis. Epithelium, characterised by densely packed cells, relies on sufficient cell adhesive properties for its maintenance. This underscores the importance of changes in tissue interactions between cells and the ECM (both cell-to-cell and cell-to-ECM adhesion) for tissue transformation (Huttenlocher & Horwitz, 2011; Khalili & Ahmad, 2015). The main function of cell adhesion in morphogenesis is the guidance of cellular behaviours through adhesion molecules, providing anchorage points and directional cues. Additionally, by forming adhesive contacts with neighbouring cells, epithelial cells can transmit signals that coordinate their behaviour. Changes in adhesion molecule expression, localization, and activity drive epithelial cells to undergo specific morphogenetic processes, including epithelial-to-mesenchymal transition (EMT), mesenchymal-to-epithelial transition (MET), and branching morphogenesis, facilitating developmental events. In this sense,

adhesion is not merely a means of sticking cells together; it is a dynamic and regulatory mechanism that influences almost every aspect of tissue morphogenesis. (Barone & Heisenberg, 2012; Gumbiner, 1996).

Concurrently, the actin cytoskeleton emerges as a central player, providing structural support and driving cellular movements that sculpt tissues (Pollard & Cooper, 2009). Along with associated proteins, the actin cytoskeleton contributes to mechanical support, serving as the primary force in morphogenesis when moved. This force is generated by actomyosin, an actin-dependent contractile complex that facilitates coordinated cell movements, shaping tissues and organs into their final forms during development. Moreover, actin polymerization drives the formation of actin-rich structures such as lamellipodia and filopodia, mediating cell motility (Svitkina, 2018). These actin-based protrusions at the leading edge of migrating cells sense extracellular cues and guide cell movement along specific paths. Additionally, actin facilitates cell fusion (Eitzen, 2003). Thus, the dynamics of the actin cytoskeleton are intricately linked to various signalling pathways, serving as platforms for the assembly and activation of signalling complexes to guide the cells during morphogenesis (Clarke & Martin, 2021).

Cell shape changes are orchestrated by several mechanisms, including elongation, constriction, and shape polarization. Elongation involves extending cellular protrusions or internally reprogramming the cytoskeleton, guided by intracellular signalling, cytoskeletal dynamics, and mechanical cues. This can cause flattening of the cells or the reverse process of columnarization, or changes of one planar axis (for example, the x-axis) at the expense of another (for example, the y-axis). In specific epithelia, apicobasal elongation changes cuboidal cells into columnar ones (Keller, 2006; Suzuki et al., 2012). Constriction of either or both surfaces may facilitate elongation. Basal and apical constriction are key processes driving cell shape change. Basal constriction involves the contraction of the basal domain, causing tissue bending and invagination, while apical constriction involves the contraction of the apical domain, aiding tissue folding and luminal narrowing (Martin & Goldstein, 2014; Suzuki et al., 2012). During constriction, processes like ingression of individual cells and EMT can occur, enabling epithelial cells to acquire a mesenchymal phenotype with enhanced migratory capacity and invasiveness (Kalluri & Weinberg, 2009). Cell shape polarization is pivotal for generating forces; without it, cells lack the ability to undergo the coordinated movements and rearrangements essential for properly shaping tissues and organs (Rappel & Edelstein-Keshet, 2017).

Lastly, an essential factor in morphogenesis is cell migration and intercalation, which are sometimes the only contributors to tissue reorganization. Without these processes, the

movement of cells or tissue to their designated positions would be impossible. Cell intercalation involves neighbouring cells exchanging places, occurring within a single plane (lateral) or between adjacent planes (radial), leading to tissue elongation or narrowing (Walck-Shannon & Hardin, 2014). Cells can migrate individually or in groups, responding to extracellular signals like chemical or mechanical gradients. Directed migration depends on dynamic cytoskeletal rearrangements, with protrusions at the leading edge and myosin-mediated contractility generating traction forces (Aman & Piotrowski, 2010). Collective cell migration, predominant during organogenesis and morphogenesis, features diverse shapes and organizational patterns, typically with leader cells at the forefront and followers trailing behind. Leader cells, identified by their cellular extensions oriented towards external cues, not only guide direction but also generate traction forces essential for the migration process. In collective migration, usually only a select few cells at the front exhibit these behaviours. Leader cells provide external cues to follower cells, which, in turn, cooperate and actively contribute to the generation of forces. This constructive collaboration between leader and follower cells ensures coordinated and efficient movement of cell groups (P. Lu & Lu, 2021).

These previously mentioned primary mechanisms collectively contribute to morphogenesis, a fundamental process in developmental biology. No single process alone can drive major changes; instead, developmental events are orchestrated through the coordinated action of multiple interlinked mechanisms. This coordination triggers a cascade of morphogenetic processes, ultimately culminating in the formation of complex organs and structures.

1.1.4. Fusion of Epithelia

The fusion of epithelia involves the seamless integration of distinct epithelial layers to form a unified structure. Epithelial fusion is a common phenomenon utilized in various processes in *Drosophila*, with examples including wound healing, dorsal closure, and the fusion of epithelial sheets derived from separate imaginal discs during metamorphosis. The fusion process involves the presence of filopodia originating from the leading edge of the fusion, whether it is from single cells, a group of cells, or the entire cell sheet edge. The role of filopodia is to establish contact with the cells prior to the joining event (Fristrom, 1988). Interestingly, cells at the leading edge of the fusion process, which contact cells of the other epithelium, are partially mesenchymal because they lack adherens junctions at their free edge (Leggett et al., 2021).

The fusion process is orchestrated by a complex interplay of molecular signals, cellular rearrangements, and mechanical forces. Initially, epithelial cells, from adjacent tissues, undergo coordinated movements, guided by chemical cues and cell-cell adhesion molecules. As the two epithelial layers approach, specialized cellular protrusions facilitate initial contact and adhesion. Subsequently, cell-cell recognition molecules mediate tight adhesion between the side-by-side membranes, leading to the formation of stable intercellular junctions. Cytoskeletal rearrangements drive cell shape changes and membrane remodelling, facilitating the merging of the epithelial layers. This fusion process is finely regulated to ensure precise spatial and temporal coordination, ultimately culminating in the establishment of fused functional epithelial structures essential for correct formation of tissue (Jacinto et al., 2001).

Parallels can be drawn between the extensively studied artificially induced epithelial movements of wound repair and the naturally occurring epithelial movements involved in organ shaping during morphogenesis. With this comparison in mind, during epithelial repair, alterations in cell shape and cell rearrangements are essential for restoring the integrity and function of the epithelium. Initially, cells at the wound edge assume a migratory phenotype, while neighbouring cells undergo shape changes. Consequently, cells surrounding the wound undergo a transition from a static morphology to a more elongated migratory phenotype, facilitating efficient migration towards the other side of the wound, which aids in the fusion process. As cells migrate and rearrange, they establish new cell-cell contacts and junctions, forming a continuous epithelial layer across the wound. Another movement during wound repair, known as zippering, involves the coordinated fusion of adjacent epithelial sheets, starting from a single point and progressing along the wound, reminiscent of a zipper on a jacket. Initially, specialized cell protrusions extend from the leading fusion cells, establishing initial contacts with the opposing epithelium and initiating adhesion and signalling events. As zippering advances, adherens junctions and tight junctions between adjacent cells strengthen, promoting stable cell-cell interactions (Fujisawa et al., 2019; Jacinto et al., 2001; H. Lu et al., 2015).

1.2. *Drosophila* Head Morphogenesis

1.2.1. Eye-Antennal Imaginal Discs, Larval Precursor of Head Structure

In holometabolous insects like *Drosophila*, which undergo complete metamorphosis, the precursors of most adult structures of the head, thorax, and legs are maintained during larval

stages as distinct clusters of undifferentiated cells called imaginal discs. The name refers to the final, adult stage of insect development, which is classically known as the imago. The head cuticle is formed by the clypeo-labral, labial, and eye-antennal imaginal discs, although most of the head capsule and major head related sensory organs derive from the eye-antennal discs (Haynie & Bryant, 1986). That is the reason this bachelor's thesis focuses on the eye-antennal imaginal discs to study the formation of the head.

The imaginal discs are thought of as larval structures, but the initial specification of eye-antennal imaginal discs occurs during early embryogenesis. The cells needed for the two eye-antennal discs of each developing fly are derived from multiple embryonic segments that migrated to form the pair. The developing eye-antennal disc becomes visible as a single unit for the first time in very late-stage embryos before hatching (B. P. Weasner & Kumar, 2022; Younossi-Hartenstein et al., 1993). At the start of the first larval stage (L1), the eye-antennal epithelium consists of a small number of undifferentiated cells with limited indications of regional patterning. By the end of the third instar larva (L3), the disc is comprised of about 45 000 cells, and the eye-antennal disc is subdivided into two major morphogenetic fields (eye and antenna), each containing multiple primordia (Figure 1). The eye morphogenetic field includes separate primordia for eye, cuticle, and ocelli, whereas the antennal field includes different primordium for antenna, maxillary palp, and cuticle. The eye and antennal fields can be distinguished based on morphology in L3 and are sometimes considered separate discs at this stage (Kenyon et al., 2003).

Although the pair of eye-antennal discs was initially referred to as a simple monolayer sheet of epithelial cells, it has a more complex morphology, including diverse cell shapes, types, and organization. Traditionally, it is described as a sac-like structure with the apical sides toward the lumen, consisting of three distinct cell layers (Figure 1C): a columnar pseudostratified epithelium called the disc proper (DP), squamous cells called the peripodial epithelium (PE), and cuboidal cells called the margin (M). Each of these distinct parts has a specific role. The two epithelial layers are joined together along their edges by the M cells; thus the 3 layers enclose a thin lumen. The DP develops into the adult sensory organs, including eyes and antennae (Gibson & Schubiger, 2000; B. P. Weasner & Kumar, 2022). The PE is thought to function primarily during metamorphosis in disc fusion and eversion, after which it would be eliminated (Fristrom & Fristrom, 1993). For instance, during L3 to pupa development, disruption of the PE prevents eye disc eversion and alters the normal morphology of the discs, suggesting that the PE actively contributes to fusion by providing the force needed for disc movement (Milner et al., 1983, 1984). Additionally, PE signalling is essential for regulating

the proliferation of the DP and ensuring DP cell survival (Gibson & Schubiger, 2000). It also directly influences the cell numbers in the DP by producing progeny that become part of the DP (Pallavi & Shashidhara, 2003). Although eye-antennal imaginal discs undergo various morphological changes during larval-to-adult development, much of our knowledge about their morphogenesis is derived from observations made before pupariation, during the embryo to L3 developmental stage, and fate mapping due to the difficulty of observing the eye-antennal imaginal disc *in vivo*.

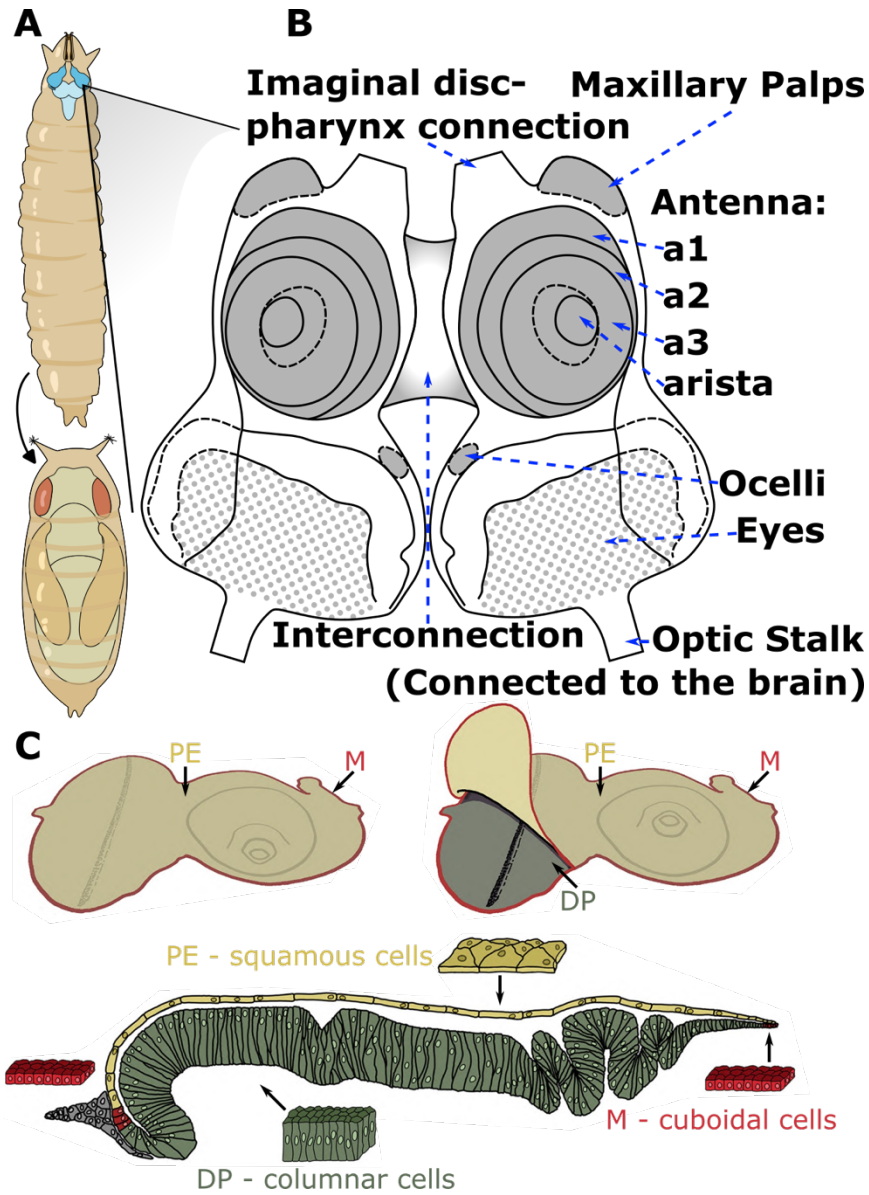

Figure 1. *Drosophila* melanogaster eye-antennal imaginal discs. (A) The positioning of the eye-antennal imaginal discs in the larva determines the position of the head capsule in the adult. (B) A pair of eye-antennal discs is connected by an interconnection. Under a microscope, two distinct regions can be observed: the antennal region, consisting of segments a1, a2, a3, the arista, and the eye region. a1, a2, a3 are first, second, and third antennal segments, respectively. Ocelli and maxillary palps, while not distinguishable under the microscope within the eye-

antennal disc, are confirmed to be present through the use of antibodies and fate maps (Kenyon et al., 2003). (C) The eye-antennal disc comprises 3 distinct cell layers. The disc proper (DP) is a pseudo-stratified epithelium consisting of columnar shaped cells. It is covered by a similar sized sheet of squamous cells called the peripodial epithelium (PE). These cells layers are joined together along their edges by a thin layer of cuboidal cells called the margin cells (M). (Picture (C) modified from Weasner & Kumar, 2022).

1.2.2. The Missing Gap of Imaging Head Development in *Drosophila*

Unlike the wing discs, much remains unknown about the development of the eye-antennal imaginal discs. One reason is lack of clear imaging larvae and pupae to observe the eye-antennal disc development. Despite significant advancements in imaging technology, specimens that exhibit high light scattering properties, such as *Drosophila* pupae, especially in the head region, remain challenging to observe with current optical imaging techniques. Additionally, the presence of muscle, fat bodies, brain, larval/pupal cuticle, and puparium complicates imaging efforts (Arranz et al., 2014).

Even with improved imaging technology, a challenge arises regarding morphogenetic movements during head formation, called head eversion, which poses difficulties in understanding. This occurs during the transition from prepupa to pupa, a crucial stage known as pupal ecdysis. During pupal ecdysis, the fly sheds its larval cuticle, inverts its head deep within the pupa, and moves tissue around, after which the head moves to become positioned outside the body. This process involves complex morphogenetic movements of the head structures, including the eye-antennal imaginal discs. The complexity arises from the need to follow the coordinated extension, inversion, and invagination of tissues in the head structure, leading to the outward protrusion of the head structures from the pupal surface. While extension and invagination are easier to follow, inversion is especially challenging, involving the turning of imaginal discs inside out. Prior to inversion, the basal surface of the imaginal discs faces the outside environment, while after pupal ecdysis, the apical surface of the adult cuticle faces outer the environment (Fagotto, 2015; Pesch et al., 2016). Pupal ecdysis marks the completion of the transformation initiated at pupariation, transitioning from a larval-shaped to an adult-shaped pupa. Simultaneously, the head cuticle, which previously resembled that of a worm, transforms into a rudimentary adult-looking fly head. After pupal ecdysis, the *Drosophila* head undergoes the acquisition of bristles and head-related organs, such as the proboscis, ocelli, maxillary palps, and antennae, which were previously absent (Elliott et al., 2021; Hartenstein, 1993; Lahr et al., 2012).

1.2.3. Adult Head Structures

Drosophila head, located at the most anterior end of the insect's body, constitutes a rigid and highly sclerotized compact structure with bilateral symmetry. Comprising six segments fused together to from a head capsule, these segments primarily arise from the fusion of two independent eye-antennal imaginal discs. These segments include four postoral sections, which contribute to the formation of the maxillary palps, proboscis, labium, and labellum, all surrounded by cuticle (Figure 2). Additionally, there are two preoral structures that form ocular organs and antennae, also surrounded by cuticle (Rogers & Kaufman, 1996).

Positioned dorsally in the adult head are a pair of ocelli, simple eyes primarily sensitive to light intensity and direction, surrounded by arrays of sensory bristles crucial for mechanosensation and environmental detection. Located ventrally, the head comprises mouthparts, including the maxillary palps and proboscis, which terminate with the labellum, a specialized organ for taste perception. prominently featured laterally are the compound eyes, while anteriorly, the head features a pair of antennae segmented into three proximal segments (a1-a3), which terminate with a distinguishable slender sensory bristle known as an arista (ar). Functioning as multifunctional sensory organs, these antennae detect olfactory and tactile cues (Cumming & Wood, 2017; Royet & Finkelstein, 1995; Todi et al., 2004). As mentioned above, the development of the head involves three separate imaginal discs. Among these, the eye-antennal imaginal discs play a significant role in the formation of various head structures, including the upper proboscis, maxillary palps, ocelli, head capsule, antennae, and compound eyes. In contrast, other head structures such as the labium and labellum originate from different imaginal discs, namely clypeo-labral and labial disc respectively (Hartenstein, 1993).

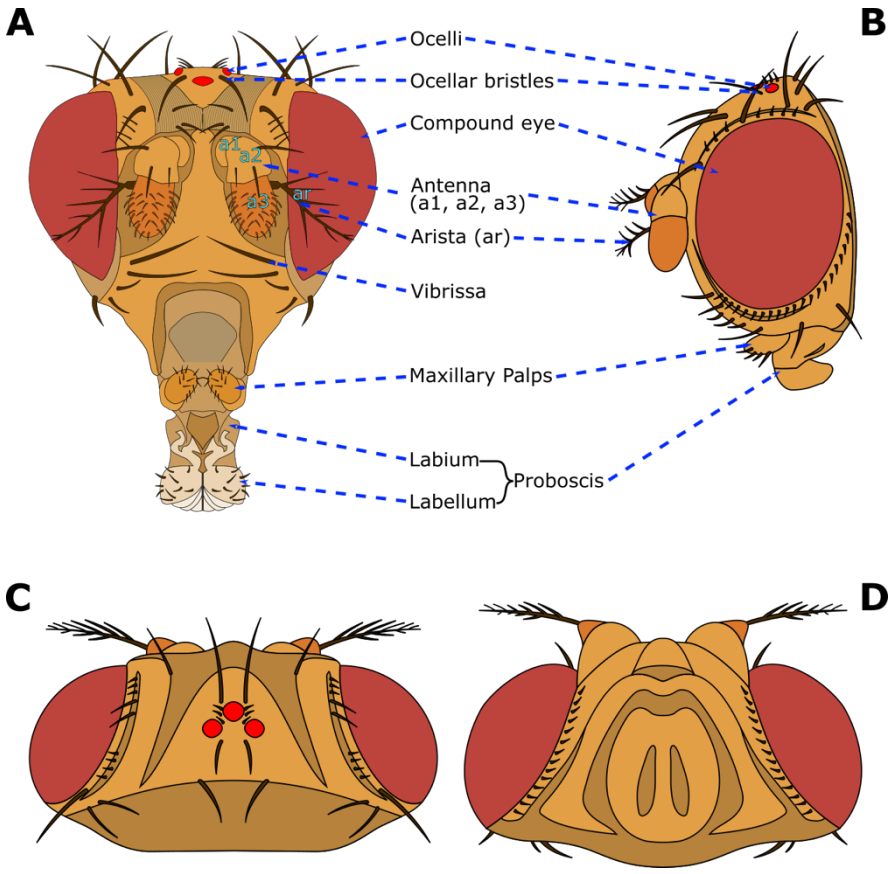

Figure 2. Anatomy of the adult head of *Drosophila melanogaster* at different angles. (A) Anterior view of the head. Reporter analysis suggests that the cuticle beneath the eye, the second antennal segment, the vibrissae and the maxillary palps contains cells that are derived from the peripodial epithelium (Atkins & Mardon, 2009). The labium and labellum are derived from the clypeo-labral disc and labial disc respectively. Adult head in the (B) lateral, (C) dorsal, and (D) ventral views. a1, a2, a3 and ar are first, second, and third antennal segments and the arista, respectively.

1.3 *Drosophila* Head as an Ideal Model for 3D Morphogenesis

1.3.1 Advantages of Using *Drosophila* as a Morphogenesis Model

Drosophila stands out as an ideal model for studying morphogenesis for several compelling reasons. Firstly, its well-established status as a model organism and its genetic manipulability provides a powerful toolkit for genome manipulation, allowing for precise experimental control. Secondly, the remarkable evolutionary conservation of developmental pathways and mechanisms between *Drosophila* and higher organisms, including humans, is noteworthy. Approximately 60% of the fly genome is homologous to that of humans, with a significant overlap in disease-related genes, estimated at around 75% (Mirzoyan et al., 2019). Insights gained from studying morphogenesis in *Drosophila* often have direct relevance to

understanding human development and disease. Despite its small size, *Drosophila* possesses complex organ systems with well-defined anatomy, making it comparable to higher organisms. Notably, the low cost, minimal resource requirements, speed of experiments, and distinct stages of morphogenesis make *Drosophila* particularly advantageous for studying morphogenesis in various laboratory environments compared to other model organisms.

1.3.2. Genetic and Molecular Tools Employed in *Drosophila*

Drosophila's well-established genetic toolkit provides ease of manipulation for various experiments. The Gal4/UAS system is particularly advantageous, allowing for spatially restricted transgene expression research. Over the years, this system has been modified countless times, enabling researchers to generate mutant cells and tissues in a spatially and temporally controlled manner, with systematic screening of *in vivo* mutants achieved through RNA interference (RNAi) or gene overexpression (Barwell et al., 2017; Brand & Perrimon, 1993).

The Gal4/UAS system consists of two main components: a gene encoding the yeast transcriptional activator Gal4, and a binding region called the upstream activation sequence (UAS). Gal4 alone has little to no effect, as its primary role is to bind to the UAS region, which is either absent or poses no harm in wild-type flies. Since Gal4 by itself does not produce a phenotype change, it is necessary to combine it with a UAS-containing transgene. By placing Gal4 under the control of a tissue-specific promoter and using a UAS-containing transgene to express the gene of interest, researchers can direct spatial expression of the specified gene (Brand & Perrimon, 1993; Osterwalder et al., 2001). If the Gal4/UAS system fails to produce a distinct phenotype or if the signal of the target gene needs observation, a specific reporter gene must be linked to the UAS-containing transgene. The most commonly used reporter gene is green fluorescent protein (GFP); however, for a multi-colour system, other reporter genes can also be effectively utilized. This linkage allows for precise localization to be identified (He et al., 2019).

The ability to control the temporal activity of the Gal4/UAS system is quite limited, as most Gal4 promoters are active across multiple developmental stages or throughout the entire fly life cycle. To address this temporal constraint, the temperature sensitive Gal80 (Gal80ts) was developed, facilitating the creation of conditional knockdown or overexpression experiments. Normally, Gal80 functions as a repressor of Gal4 in yeast. The Gal80ts variant was engineered to function normally at 18°C, binding to Gal4 and restricting its interaction with UAS.

However, at 29°C, Gal80ts dissociates from Gal4, allowing the activation of the gene of interest. The utilization of this extended GAL4/UAS/GAL80ts system enables precise control and regulation of gene expression in a spatiotemporal manner (Barwell et al., 2017; McGuire et al., 2003).

Another tool widely employed in *Drosophila* research is FLP-FRT recombination, a site-directed recombination technology used to precisely manipulate an organism's DNA under controlled conditions. This technology, originating from yeast, consists of two essential components: one is a recombinase called flippase (FLP), the other is the flippase recognition target (FRT). The initial adaptation for using this system in research involved integrating it with a heat shock promoter. This allowed temperature control of FLP, with recombination activated at 37°C. However, due to its lack of specificity, this led to the generation of mutant clones throughout the entire organism (Golic & Lindquist, 1989). Subsequent modifications have allowed for direct control by specific regulatory elements or indirect coupling to genomic enhancers using the Gal4/UAS system, enabling a more specific generation of mutants (B. M. Weasner et al., 2017). Depending on its application, FLP-FRT recombination technology can produce diverse outcomes.

One such application is lineage tracing using trans-chromosomal recombination. This process induces recombination specifically during the G2 phase of the cell cycle, resulting in the creation of two sibling clones, which in epithelia typically remain in close proximity. As the mechanism relies on sister chromatid exchange, it occurs exclusively in mitotically active cells. Some examples of this approach include the G-trace methods. The G-trace method allows for the simultaneous comparison of real-time expression patterns in newly formed cells, for example, they give a GFP signal, while historical expression signals are present in older activated cells, for example, emitting an RFP signal (Evans et al., 2009; H.-H. Yu et al., 2009). Alternative methodologies include loss-of-function clones employing cis-chromosomal recombination, where FLP triggers recombination between FRT sites oriented in the same direction. This process results in the excision of the DNA sequence situated between the FRT sites (FRT cassette), generating "mutant" cells distinct from the original environment of original cells. Notably, this type of excision is heritable and can occur at any phase of the cell cycle, ensuring that all cell offspring inherit the "FLP-out" genotype (Germani et al., 2018). Furthermore, this approach can also be used to overexpress the gene of interest. Instead of truncating the gene of interest, FLP excises the stop codon positioned within the FRT cassette. Consequently, the removal of the FRT cassette facilitates gene expression. Similar to loss-of-

function clones, this recombination is heritable and can occur at any stage of the cell cycle (Pignoni & Zipursky, 1997; Tanguay & Morrow, 2008).

Several more advanced methods have been developed, leveraging different components of FLP-FRT, extended with Gal4/UAS and other systems. One such development led to the creation of CoinFLP. This system enables the generation and comparison of two mutant cell populations within a single tissue. A specialized version of CoinFLP was engineered to incorporates both Gal4/UAS and LexGAD-LexAop systems. The latter functions similarly to the Gal4/UAS system, with LexAop (similar to UAS) serving as the binding site for LexGAD (similar to Gal4), a transcriptional activator, to express the gene of interest. These two systems function independently; Gal4 exclusively activates the UAS gene, while LexGAD interacts solely with LexAop. Additionally, the CoinFLP system utilizes two distinct FRT sites: FRT and FRT3. Between FRT, there is only a stop cassette, while between FRT3, there exists both a stop cassette and the LexGAD transcribing gene. This means that the modified gene consists of a stop cassette, downstream of which is LexGAD, followed by Gal4 (Bosch et al., 2015).

FLP recombination of FRT leads to the excision of the stop cassette This results in the expression of LexGAD, which activates the gene downstream of LexAop (GFP). Recombination between FRT3 sites leads to the excision of both the stop cassette and LexGAD. The removal of the stop cassette causes the expression of Gal4, which activates the gene downstream of UAS (RFP). The choice of FRT is random, and only one FRT can be excised within the cell, hence the term CoinFLP. This mechanism generates mosaic tissue within a single tissue, with some patches expressing Gal4 (RFP) and others expressing LexGAD (GFP). (Bosch et al., 2015).

1.3.3. *Ex vivo* Approaches in *Drosophila*

Despite the enormous potential of imaginal discs as a model system, live imaging for certain experiments poses technical challenges due to the necessity of larval immobilization and the deep-seated location of the imaginal discs within the organism. While live imaging is feasible for some discs within a limited time window, *ex vivo* culture techniques have been explored since the 1960s to address these hurdles (Schneider, 1964).

Ex vivo culture enables high-resolution analysis of developmental dynamics in a controlled environment. Manipulation of various genes or factors within the growth medium allows researchers to conduct experiments that are challenging *in vivo*. Importantly, comparison of *ex vivo* with *in vivo* conditions reveals similar developmental patterns in flies, which can support

each other and aid researchers in making new discoveries. Thus, *ex vivo* setups have facilitated detailed observation of tissue growth and patterning effects, real-time imaging of dynamic cellular behaviours, and examination of gene expression patterns during morphogenesis (Tsao et al., 2016; Xu et al., 2021).

Ex vivo protocols for studying *Drosophila* imaginal discs have long served as powerful experimental tools. In contrast to mammalian tissues, most *Drosophila* organ cultures can only be sustained *ex vivo* for about a day, indicating gaps in our understanding of the culture conditions required to fully support explanted *Drosophila* tissues. One of the most pressing challenges is identifying a culture medium that can sustain the growth and development of the imaginal discs over an extended period. Fortunately, a chemically defined medium designed to mimic larval haemolymph composition has been developed allowing for some understanding. Testing for optimal culture conditions using cells derived from imaginal discs revealed that the addition of insulin and 20-hydroxyecdysone improved cell survival rate and proliferation (Marchetti et al., 2022). The steroid hormone 20-hydroxyecdysone regulates processes such as cell specification, differentiation, and apoptosis. Concentration peaks of this hormone orchestrate crucial developmental events, including larval and pupal moulting stages, as well as the initiation of imaginal disc development (Riddiford & Truman, 1993). Without this ecdysteroid and insulin, *ex vivo* cultures fail to undergo differentiation.

While numerous *ex vivo* experiments have been conducted on the brain and wing discs of the fly, relatively few studies involve eye-antennal imaginal discs due to challenges associated with their acquisition, long-term culturing, and observing developmental stages (Kumar, 2018).

1.4. Introducing Head Morphogenesis as a Model System

The *Drosophila* eye-antennal imaginal discs serve as an attractive model system for investigating epithelial patterning and morphogenesis. Biological processes such as cell-neighbour rearrangement, apical/basal constrictions, and other cell shape changes and migrations observed during *ex vivo* head formation are conserved across various developing epithelial tissues, suggesting that insights gained from this system have wide-ranging applicability. This unique *ex vivo* head formation system offers a new opportunity for three-dimensional research, unlike other *Drosophila* models that are more studied or represent two-dimensional systems.

The *ex vivo* head formation system serves as a well-developed model for investigating tissue formation, as there exists a basic framework for understanding key processes. This framework

includes detailed insights into the development of eye-antennal imaginal discs, understanding of the involved components, and the mechanisms underlying fusion. The potential for discoveries and application of other *Drosophila* species in the fusion process *ex vivo* further enhances the significance of this system in expanding our understanding of development.

2. EXPERIMENTAL PART

2.1. Aims of the Thesis

This project aims to develop an *ex vivo* culture method to track head morphogenesis in real-time using 5D imaging, which encompasses dimensions of XYZ, time, and wavelength. By employing this method, the project seeks to achieve a detailed, step-by-step understanding of the transition from third instar larval eye-antennal imaginal discs to the pupal head eversion stage, elucidating the crucial steps necessary for progressing to subsequent developmental stages. Additionally, the project endeavours to explore the molecular mechanisms underlying the fusion process.

2.2. Materials and Methods

2.2.1. Fly Stocks and Genetics

This study of head morphogenesis has been facilitated by the accessibility of genetic tools and techniques. Numerous *Drosophila* lines have been created for various aspects of *Drosophila* research and are available from stock centres. The current project owes its progress to the diverse array of fly lines and tools obtained from the Bloomington *Drosophila* Stock Center (https://bdsc.indiana.edu/index.html) and the KYOTO Stock Center (https://kyotofly.kit.jp/cgi-bin/stocks/index.cgi). Determining the precise genotype is crucial for each separate experiment, leading to the utilization of various fly lines for specific purposes (Table 1). These fly lines employ a variety of mechanisms, including UAS/Gal4/Gal80ts, FLP-FRT, heat-shock induction, balancer chromosomes, and gene manipulation techniques such as overexpression, knockout, or knockdown.

Table 1. List of fly lines used in the thesis.

Organism/strain	Source	Identifier	Purpose
yw; act-Gal4 (III)	N/A	N/A	Highly conserved proteins, ubiquitously expressed in all eukaryotic cells

Caspase sensitive Gal4/CyO	N/A	N/A	Identify cells with ongoing or past caspase 3 activity
y[1] [w*]; M{w[+mC]=Ubi-GFP-CAAX}ZH-86Fa	KYOTO	109823	Ubiquitously expressing a membrane-bound GPF, located on the 3rd chromosome
y[1] w[*]; M{w[+mC]=Ubi-GFP-CAAX}ZH-22A	KYOTO	109824	Ubiquitously expressing a membrane-bound GPF, located on the 2nd chromosome
y[1] w[*]; M{w[+mC]=Ubi-TagRFP-T-CAAX}ZH-22A	KYOTO	109825	Ubiquitously expressing a membrane-bound RFP
y[1] w[*]; P{w[+mC]=His2Av-mRFP1}III.1 M{w[+mC]=Ubi-GFP-CAAX}ZH-86Fa	KYOTO	109829	Simultaneous imaging of ubiquitously expressing a membrane-bound GPF and the chromosome (RFP)
w[*]; M{w[+mC]=Ubi-GFP-CAAX}ZH-22A P{w[+mC]=His2Av-mRFP1}II.2	KYOTO	109830	simultaneous imaging of ubiquitously expressing a membrane-bound GPF and the chromosome (RFP) (stronger RFP signal)
P{ry[+t7.2]=hsFLP}12, y[1] w[*]; sna[Sco]/CyO	Bloomington	1929	Expresses Flp recombinase upon heat shock.
w[*]; P{w[+mC]=UAS-RedStinger}4, P{w[+mC]=UAS-FLP.D}JD1, P{w[+mC]=Ubi-p63E(FRT.STOP)Stinger}9F6/CyO	Bloomington	28280	Allows analysis of real-time and lineage-traced expression of GAL4 drivers together with Caspase sensitive Gal4
w[1118]; P{w[+mC]=UAS-GFP.nls}14	Bloomington	4775	Expresses nuclear localized GFP under the control of UAS
w[*]; P{w[+mC]=UAS-p35.H}BH1	Bloomington	5072	Expresses the baculovirus p35 cell death inhibitor under UAS control

y[1] w[*] P{y[+t7.7] w[+mC]=10XUAS-IVS-mCD8::RFP}attP18 P{y[+t7.7] w[+mC]=13XLexAop2-mCD8::GFP}su(Hw)attP8; P{y[+t7.7] w[+mC]=CoinFLP-LexA::GAD.GAL4}attP40	Bloomington	58754	CoinFLP imaging toolkit. Expresses mCD8-tagged GFP under the control of 13 LexA operator sequences. Expresses mCD8-tagged RFP under the control of 10 UAS sequences with an intron (IVS) interposed between the UAS and coding sequences. Overlapping FRT cassettes allow irreversible clonal choice between Gal4 or LexA expression upon Flp recombination.
w[*]; P{w[+mC]=UAS-mCherry.CAAX.S}2	Bloomington	59021	Expresses membrane-targeted mCherry (RFP) under UAS control.
y[1]; P{w[+mW.hs]=GawB}c311	Bloomington	5937	Expresses Gal4 in eye disc peripodial epithelia
sd[12] P{ry[+t7.2]=neoFRT}19A/FM6; P{w[+mW.hs]=GawB}mirr[DE]/TM6B, Tb[1]	Bloomington	78371	DE-Gal4, which in the eye is expressed in the dorsal compartment for most of the development, manipulate gene expression in half of the developing eye

2.2.2. Culture Media Compositions

For both the dissection and preparation of the culturing stock media, we employed Shields and Sang M3 Insect Medium (Sigma S8398). This was prepared by combining 0,5 g KHCO3 and M3 Insect Medium powder (Sigma S8398) in 1000 mL of ddH_2O (Milli-Q) water. 100 mL of this solution was reserved for dissections (M3 dissection media), while the remaining 900 mL was used to prepare the culturing stock media (M3/IMS growing stock media) by mixing it with 100 mL of Insect Medium Supplement (Sigma I7267, 10X stock solution) and 10 mL of Penicillin-Streptomycin (Sigma P4333; final concentration 100 U/mL Penicillin, 0,1 mg/mL

Streptomycin). Both the M3 dissection media and M3/IMS growing stock media were kept under sealed, sterile conditions at 4℃ and used within three months.

Prior to experimentation, the M3/IMS growing stock media was aliquoted into 50 mL Falcon tubes and supplemented with 63 µL of Insulin (final concentration 25 µg/mL) and 25 µL of 20-Hydroxyecdysone (Sigma H5142; final concentration 1 µg/mL), making up a total volume of 50 mL with the M3/IMS growing media. Aliquots (M3/IMS growing media) were used within one or two weeks, and no changes in the quality of the media were observed. Ecdysone was stored in a stock solution of 2 mg/mL in ethanol at -20°C, while insulin was stored in a stock solution of 20 mg/mL at -20°C.

2.2.3. Dissection and Imaging

The larvae predominantly used in this study were the late third instar larvae that had undergone wandering behaviour, meaning the larvae were moving away from their food source, and becoming immobile. Late third instar larvae were washed in sterile PBS and then disinfected in 70% ethanol for less than 1 minute. After rinsing, they were briefly air-dried in a sterile environment, before being placed in a M3 dissection media, where the discs were carefully dissected using forceps and scalpels. Wounded discs were discarded, and the unharmed discs were transferred to a 35 mm petri dish filled with M3/IMS growing media, supplemented with Ecdysone and Insulin. The discs were then positioned carefully with forceps to ensure they remained within the camera's field of view. The cultured discs were observed under a stereo microscope (2.2.4. Microscopy) for approximately 1-2 hours to monitor ongoing development before further experimentation. During the monitoring process 4 to 10 disc pairs, depending on the experiment's difficulty, were imaged simultaneously. After monitoring, only one pair was selected for subsequent live imaging to ensure better quality, while the others were left in the culturing media as backups.

The dissection process involved placing the larva in a drop of 2-3 mL of room temperature, filtered, and sterile M3 dissection media on a clean silicon pad. The larva remained fully submerged in liquid throughout the entire dissection process. The eye-antennal discs were isolated from the body within 5 minutes. To separate the head region from the body, one pair of forceps grasps the mandibles and gently pulls them away, while another pair of forceps stabilizes the body. As the mandibles are pulled, the structure complex consisting of the mouthparts, eye-antennal imaginal disc, brain, and leg discs becomes visible. By continuing to pull, the head region is severed, and the body can be discarded. Care was taken not to sever the

gut to prevent bacteria from entering the media. The cuticle surrounding the mandibles is then removed to facilitate the location of other body parts. The leg discs are extracted from beneath the brain, followed by the removal of the wing disc if necessary. To ease the cutting of the optic stalk connecting the brain to the eye-antennal discs, the brain is gently pulled away, making it easier to observe the optic stalk and detach the brain. Finally, the connection between the mandibles and the eye-antennal imaginal disc is severed. Additional cuts are made, if necessary, to tidy up tissue connected to the discs before transferring the eye-antennal imaginal discs into a 35 mm petri dish filled with M3/IMS growing media, supplemented with Ecdysone and Insulin.

2.2.4. Microscopy

We used four different microscopes: a Leica M165 FC Fluorescent Stereo Microscope, an upright microscope for checking the initial development of the discs; an Olympus IX81 Fluorescent Microscope, an inverted DIC microscope used for live imaging DIC and fluorescent experiments; a Leica Stellaris 8, a confocal microscope; and a Leica TCS SP8 STED 3X CW 3D, an inverted confocal microscope. Both confocal microscopes were used for 3D live imaging. Exact settings varied depending on the experiment and system. They were chosen to balance the need for a clear image with minimizing laser exposure to avoid tissue damage. Typically, we captured between 60 and 150 z-sections with the confocal microscopes, at intervals of 1 μm. The maximum number of z-sections taken was 250. Live imaging pictures were captured every 10 minutes. We analysed the images using various software tools, including Image J and Imaris.

2.2.5. Central PE cell area analysis

To analyse the average cell area change in the central PE, we defined the central PE subsection area. In image analysis software, the central PE area consists of flat cells with large surface area, making the cell boundaries easily distinguishable. This distinct area is enclosed by more compact cells, which form a C-shaped boundary around the central PE. By tracking the movement of a single cell near the lateral and central PE boundary, we defined a central PE area.

The average single cell area graph was created by analysing three different datasets of eye-antennal imaginal discs. In each experiment, 30 random cells were picked from the left disc

within the central PE and 30 from the right. The surface area of these cells was measured, and the total surface area was subdivided to determine the average single cell area change for each disc. Finally, the change in cell area was averaged across the three experiments. Standard deviation was used to calculate the 95% confidence intervals. The standard deviation was computed for the 30 randomly chosen cells, and then those results were averaged across the three experiments.

2.3. Results

2.3.1. Long Term *Ex vivo* Culture and Live Imaging of *Drosophila* Larval Eye-Antennal Imaginal Discs

2.3.1.1. A Method to Image Imaginal Disc Development *Ex vivo*

In the 1970s, Milner and colleagues conducted research to determine the necessary culture medium requirements for inducing the development of *Drosophila* eye-antennal discs through *ex vivo* methods (Milner et al., 1983, 1984; Milner & Haynie, 1979). However, at that time, no microscopes capable of generating time-lapse live imaging of imaginal discs were available. In recent years, methodologies for live imaging of *ex vivo* discs have begun to develop, but they typically involve the use of only a single disc. While the results showed that a single disc could develop for up to 7 hours in *ex vivo* media, it did not differentiate further to represent morphogenesis (Tsao et al., 2016). Therefore, we plan to enhance the live imaging *ex vivo* method by leveraging advanced microscope technology and incorporating the latest improvements in developmental biology field. This technique will enable us to examine the entire process of head morphogenesis, from the eye-antennal discs of the 3rd instar larvae (L3) to the head of the pupal stage (Figure 3).

To start, we optimized the culture medium to ensure that eye-antennal imaginal discs from the L3 could develop into the pupal stage. Through systematic experiments, we found that M3/IMS growing media, supplemented with Insulin and Ecdysone were essential components of the medium (2.2.2. Culture Media Compositions). We excluded fly extract and FBS (Fetal Bovine Serum), which are used with other *ex vivo* protocols, as they had no observable effect on disc development (data not shown). We experimented with different viscosity agents like low melting agarose to simulate *in vivo* conditions but found that they hindered the development of eye-antennal imaginal discs. Various concentrations of these agents caused the discs to cease movement. Finally, we created an adapted culture medium that supported prolonged imaging sessions of the disc pair for up to 20 hours using confocal or fluorescent microscopy, by adjusting the concentrations of key components and removing unnecessary or hindering agents (FBS, fly extract, agarose).

We selected L3 larvae that had reached a specific stage of development, where they were attached to the vial walls, displayed slow mobility, and had initiated pupariation (Figure 3). Following the correct selection, we sterilised the larvae by washing them in PBS and then submerging them in 70% ethanol. After sterilisation, we placed the larvae into M3 dissection media. Dissection was carried out in a large droplet of cold M3 dissection media placed on a

silicon pad in sterile conditions. The eye-antennal imaginal discs were quickly dissected and isolated (5 minutes per larva) and then placed inside a 35 mm petri dish filled with M3/IMS growing media, supplemented with Insulin and Ecdysone. This process was repeated multiple times to obtain several healthy pairs of eye-antennal imaginal discs, maximizing the chance of successful imaging. Once the desired number was obtained, we placed the petri dish under a stereo microscope for the initial 1-2 hours of imaging to observe if the eye-antennal discs underwent the correct developmental processes or if they had died during the dissection (Figure 3). If they appeared healthy, then we conducted our experiments in the next step.

During our optimization process, we experimented with various dissection techniques. Initially, we attempted to image the entire larval developing head complex, preserving both the mouthparts and the brain. However, this approach resulted in tissue thickening, making both the tissue and imaging blurry. Therefore, we decided to excise the mouthparts and the brain while still maintaining the interconnection between the discs. This adjustment enabled us to successfully establish *ex vivo* protocol and observe the dynamic changes occurring during the fusion of the eye-antennal discs (Figure 3).

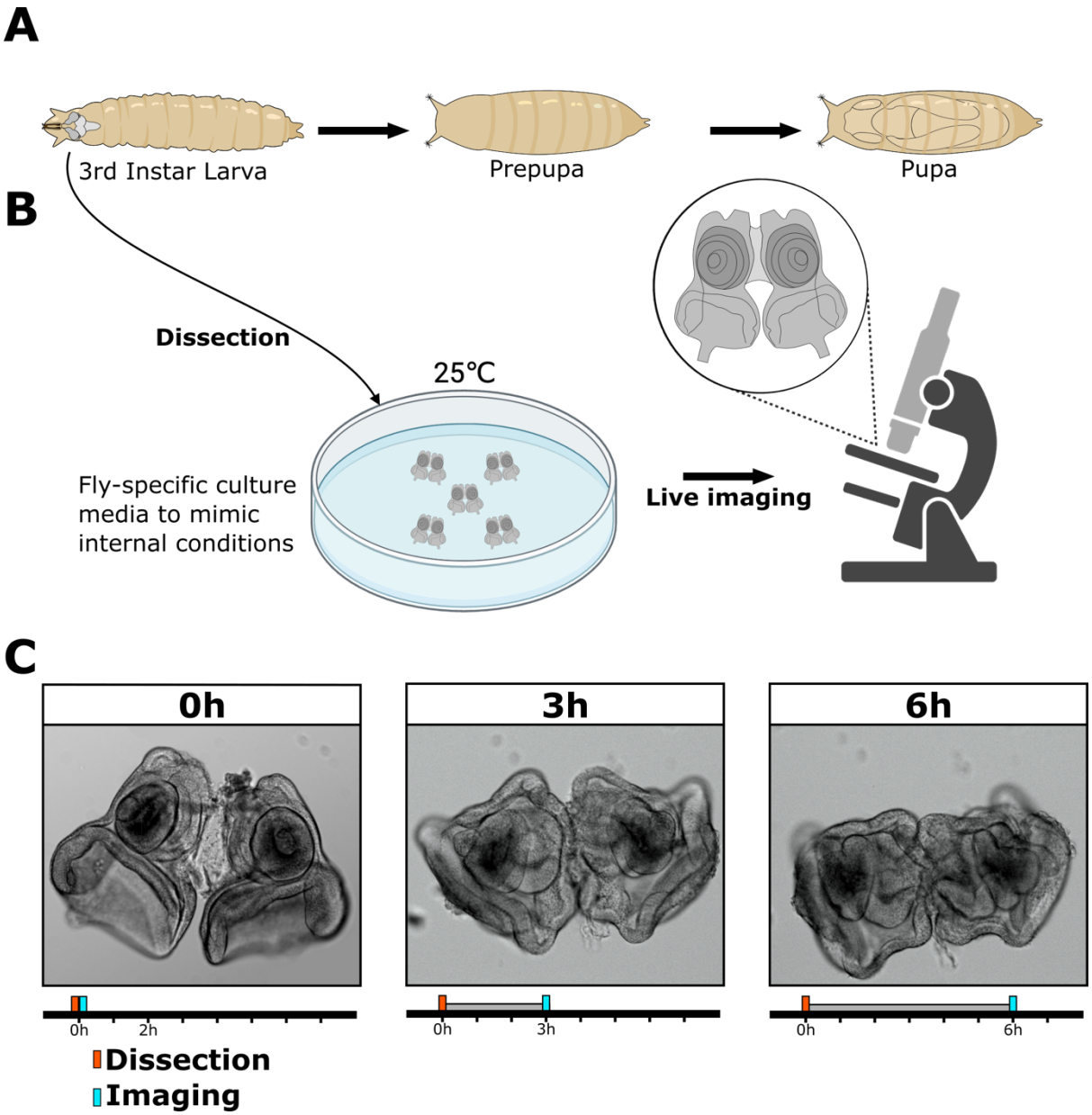

Figure 3. *Ex vivo* culture method used to observe head morphogenesis in real-time. (A) Developmental stages of a larva into pupa. First rudimentary head can be observed during the pupal stage. (B) Scheme of the *ex vivo* culturing procedure. The eye-antennal imaginal discs were isolated from 3rd instar larvae prior to pupariation and placed in the culture medium containing Insulin and the steroid hormone Ecdysone to replicate *in vivo* conditions and trigger metamorphosis, allowing for time-lapse imaging. (C) The Differential Interference Contrast (DIC) images show eye-antennal discs that were previously dissected, cultured, and then imaged. The timeline provides information regarding the timing of dissection (red box), imaging (blue box), and culturing (grey interval).

2.3.1.2. Observing Developmental Stages from 2D to 3D during *Ex vivo* Live Imaging

After establishing a modified *ex vivo* protocol, we commenced imaging procedures. While we could have extended the imaging duration to approximately 20 hours, we limited it to 14 hours to focus on understanding the development of the prepupal head (Figure 4), typically not visible

through *in vivo* imaging. Analysing the time-lapse imaging data revealed dynamic changes in individual discs and their coordination with each other. These observations led to the discovery of the fusion of two discs and the formation of a uniform structure, which was previously unknown.

In our initial time-lapse experiments, we observed dynamic morphogenetic events and coordinated fusion in two eye-antennal discs. Drawing an analogy to origami in epithelial morphogenesis, we pondered whether each individual disc must possess a specific morphology and position to align and initiate fusion. To understand the pattern of disc behaviour, we analysed five independent datasets. Our investigation revealed that between 0 to 4 hours, the most significant events that need to occur are alignment, shortening, and rotation of the discs, as observed in (Figure 4). These initial events result in rapid morphogenetic movements, distinctly observable every hour. Through these movements, the discs are pulled and positioned side by side, aligning the ocelli region and antennae on the same latitude, regardless of their initial placement. Between 5 to 9 hours, disc fusion emerges as the critical event (Figure 4). Although the pair may appear to undergo less movement compared to the previous stage, these hours mark the time of internal remodelling, transitioning from two separate discs to a singular fused complex. The final crucial event occurs between 10 to 14 hours, involving the formation of the definitive head cuticle (Figure 4). This entails the finalization of fusion and the formation of the head cuticle, an epithelium distinguishable under a microscope as covering the entire structure like a sphere.

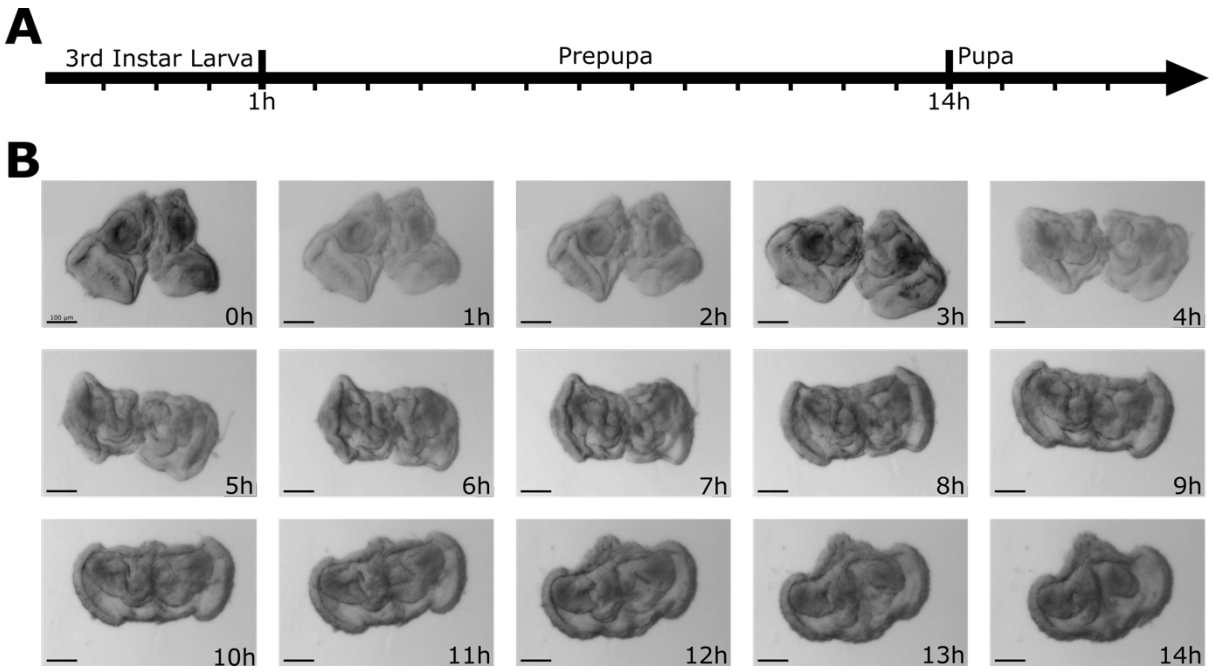

Figure 4. Time-lapse imaging of *ex vivo* eye-antennal imaginal disc. (A) Timeline describing the duration of the time-lapse, starting about an hour before the onset of pupariation and ending at the prepupa to pupa transformation (head eversion) time. (B) Time-lapse DIC images of *ex vivo* eye-antennal disc development at hourly intervals from 0 to 14 hours.

Based on our observations, each pair of eye-antennal imaginal discs exhibit similar dynamic development, allowing for their classification into four distinct stages (Figure 5). This breakdown of continuous development facilitates a better understanding of the process. The classification is established based on characteristic time-specific developmental events that consistently occur in every successful pair of *ex vivo* imaginal discs.

Stage 1 involves the shortening of the imaginal discs along the longitudinal axis, accompanied by a slight hinging of the eye field, giving the impression that the eyes are drawing closer to the antennal field. Additionally, during this stage, the interconnection between the discs pulls the discs closer to the median, and by the end of this stage, the interconnection is eliminated. This condensing process results in the eye-antennal discs aligning the antennal fields of two independent discs on the same latitude and adopting a somewhat triangular shape.

In stage 2, eyes inversion occurs, meaning that the eye field transforms from a concave to convex orientation (the eyes turn inside out). Additionally, the cuticle surrounding the antennal field completes alignment and initiates a partial fusion, making differentiation between left and right difficult, and resulting in a gradual merging of the tissue (Figure 5). The partial fusion will gradually extend towards the eye field region, resembling a zipping process.

Stage 3, called eyes rotation, involves, as the name implies, the rotation of the eye field. Previously, the eye field was rotated approximately fifteen degrees away from the median; however, during this stage, the eye field rotates to a perpendicular angle to the imaginary median symmetry axis, progressing towards its final position as it will be in the adult fly. The initial partial fusion processes have occurred between the pair of discs, resulting in difficulty differentiating left and right disc tissue near the fusion area. Between the pair of discs, near the eye field, this partial fusion creates a V-shaped furrow (Figure 5). Although the furrow persists throughout this stage, its depth decreases as cells are displaced. Consequently, some cells migrate away from the fused furrow, and round cells extrude to the surface of the epithelium. At the beginning of this stage, there are two distinct lumens, but in the end, a hole forms in the epithelium that separates the two lumens, initiating the formation of a single lumen.

During stage 4, the final fusion of the two independent discs into a continuous head complex occurs. The separating epithelium between the two discs is removed, leading to coalescence, and resulting in the formation of a single, larger lumen. The V-shaped furrow transitions into a smooth covering, finalizing the intact head capsule. Almost all differentiation between the two separate epithelia is lost. Additionally, a little later than hour 15 (during the pupal stage), it can be observed that the antennal discs rotate about 90 degrees and migrate to the middle, where the separating epithelium once was, thus allowing the antennae to touch each other.

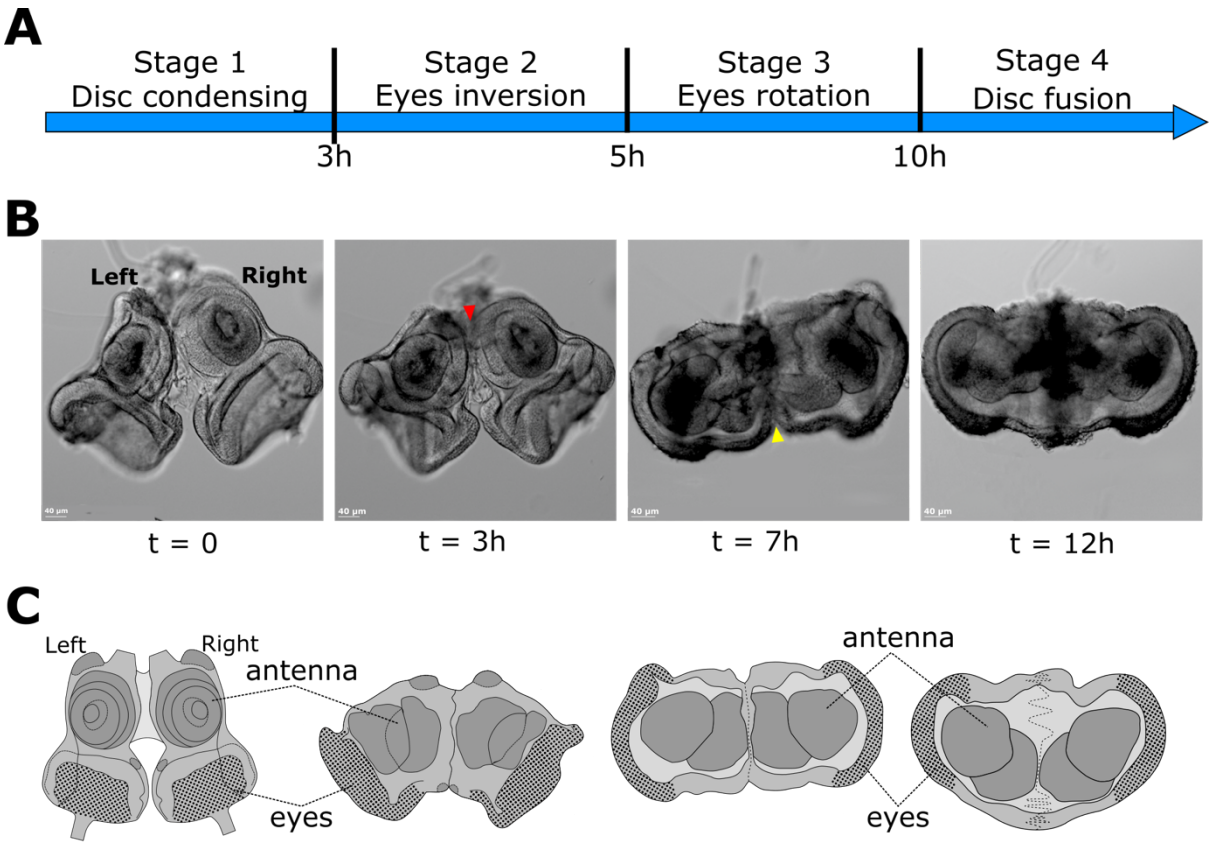

Figure 5. Overview of eye-antennal disc development. (A) Timeline characterising the stages of eye-antennal imaginal disc development, which we have divided into 4 stages: stage 1 corresponding to 0 to 3 hours, stage 2 from 3 to 5 hours, stage 3 from 5 to 10 hours, and stage 4 from 10 hours onward. (B) DIC imaging of the disc development best depicting the stages outlined in (A), showing the most characteristic morphology of each stage. The initial fusion process is highlighted by a red arrowhead, and the furrow made by said fusion is highlighted by a yellow arrowhead. (C) Schematics of the eye-antennal discs at different stages, as imaged in (B), respectively. Scale bar: (B) 200 µm.

2.3.1.3. *Ex vivo* and *In Vivo* Comparison

To ensure the reliability of our *ex vivo* methods, we aim to compare the development of eye-antennal discs during metamorphosis in both *in vivo* and *ex vivo* settings. Since following continuous major tissue remodelling is challenging *in vivo*, we dissected eye-antennal imaginal discs at different stages (*in vivo* method) and compared them at corresponding time points (*ex vivo* method) (Figure 6). To accomplish this, we selected L3 larvae of the same age and divided them into two groups: one group was dissected and cultured, while the other was allowed to pupate before dissection and imaging.

On a large scale, the cultured imaginal discs exhibit morphological changes similar to normal development. During the *in vivo* prepupal stage, no major whole-organism-related tissue

remodelling occurs, meaning that all developments occurring in the eye-antennal discs are encoded within the discs and do not require assistance from the rest of the body. Consequently, it is relatively straightforward to compare *in vivo* and *ex vivo* methods during prepupal stage, as both only require the eye-antennal discs and the information encoded within their cells. However, beyond this stage, assessing developmental similarity becomes challenging, as the pupa undergoes head eversion during the prepupa to pupa transition, a process that cannot be replicated *ex vivo*.

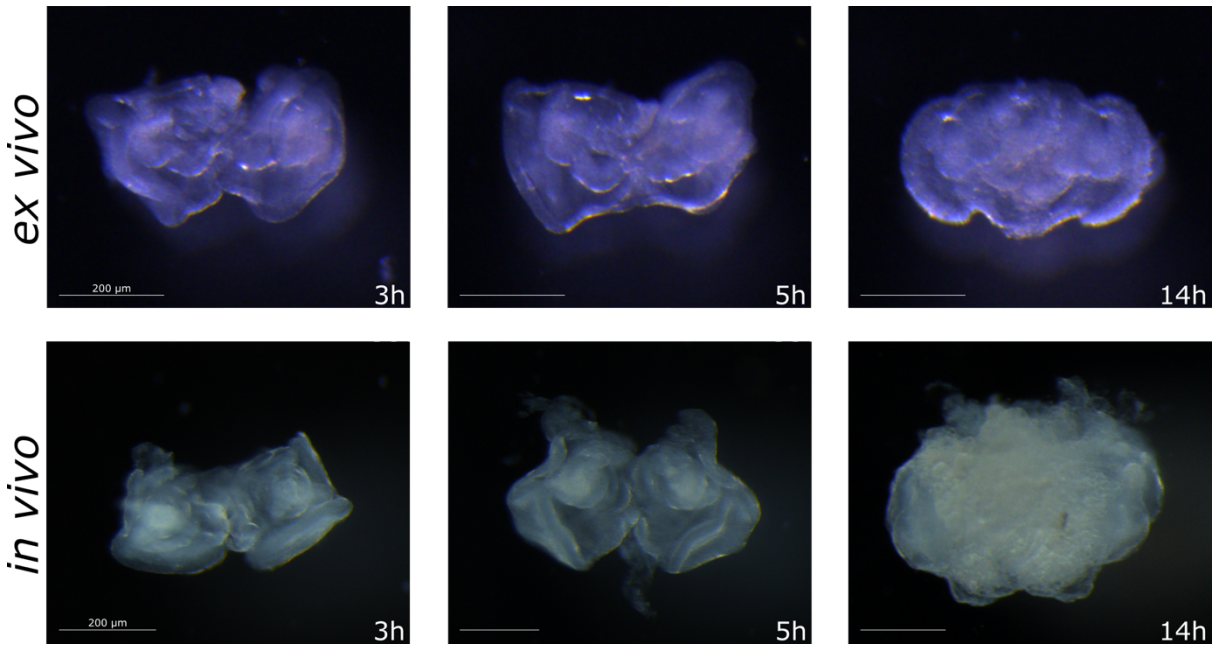

Figure 6. Comparison of eye-antennal disc morphology between *ex vivo* and *in vivo*. Early stage 2 (3 hours) and stage 3 (5 hours) *ex vivo* discs reveal a similar morphology to that found *in vivo*. However, by the end of stage 4 (14 hours) *ex vivo*, disparities become more noticeable compared to the corresponding time point *in vivo* due to extensive remodelling occurring *in vivo*. Scale bar: 200 µm.

2.3.2. Peripodial Epithelium Dynamics During the Fusion *Ex vivo* of The Eye-Antennal Imaginal Discs

2.3.2.1. PE Structures Involved in Fusion During Head Morphogenesis

We utilized this *ex vivo* approach to gain insights into the mechanisms underlying fusion. During wing imaginal disc development, the DP hosts most of the growth and cells, while the PE contributes relatively little (5%) to the cuticle of the adult fly (Tripathi & Irvine, 2022). Drawing from the wing disc model, it was considered that the PE serves as a temporary signalling structure for the DP and is subsequently eliminated. In contrast, we hypothesised

that the DP predominantly drives the development of eye-antennal discs and gives rise to all head structures.

To test this hypothesis about PE and DP, we cultured eye-antennal imaginal discs expressing membrane-bound GFP-CAAX and conducted time-lapse imaging using a confocal microscope (Figure 7, Figure 8). The live imaging data revealed that the PE layer plays a more central role in the fusion process than previously thought (Figure 7).

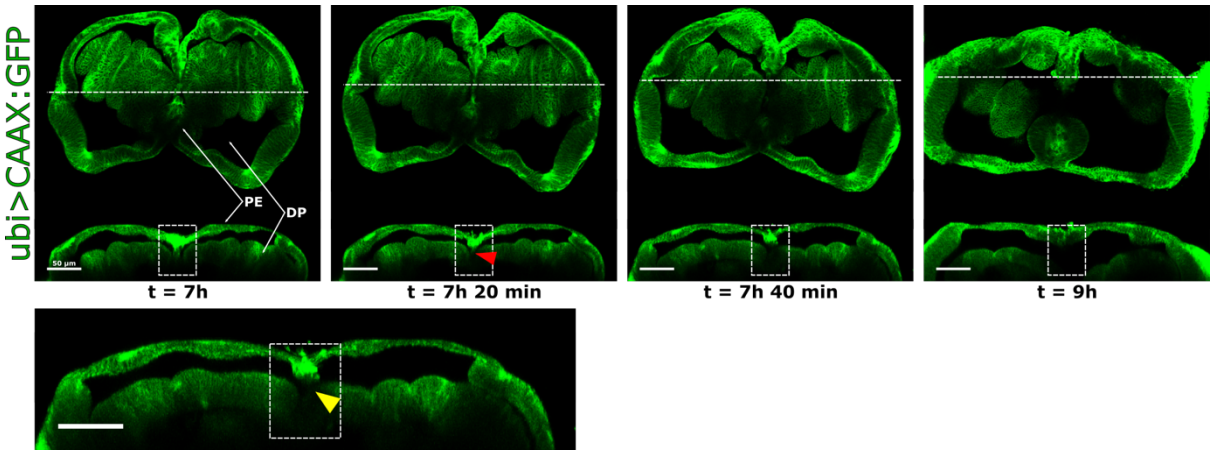

Figure 7. Fusion of the pair of eye-antennal imaginal discs visualised by ubiquitously expressing membrane-bound GFP (ubi-GFP-CAAX). Time-lapse images showing the 3D view of a pair of eye-antennal imaginal discs at 7 hours, 7 hours 20 min, 7 hours 40 min, and 9 hours after the start of culturing. The top panel displays coronal sections (upper) and transverse sections (lower) of stage 3. The dashed white line on the coronal section indicates the transverse section. The tissue fusion area is highlighted in a dashed white box in the transverse section. In the coronal view, the peripodial epithelium (PE) is positioned towards the top, and in image analysis software, a portion of the PE is intentionally cropped to facilitate better visualization of the inside of the discs. During the middle of stage 3 (7 hours), the PEs of the two separate discs merge into one, both surrounding two distinguishable lumens. After 20 minutes, an incision is made to the PE, as shown by the red arrowhead. Another 20 minutes later, the incision creates a hole between the separating PEs, and the lumens begin to coalesce. This process is more clearly depicted in the bottom panel, which showcases a transverse section with a hole between the PEs, marked by the yellow arrowhead. By 9 hours, the fusion is complete, with a single lumen, and the PE cells undergo changes in shape. DP, disc proper. Scale bar: 50 µm.

However, before delving deeper, we encountered the challenge of precisely defining the boundary between the DP and PE sides, especially with discs older than L3. Notably, our observation on the transverse sections revealed that only a small section consists of flat squamous cells, similar to the description of the PE in the literature. If we were to rely solely

on this information, it would suggest that the imaginal disc is mostly composed of DP with only a small area of PE.

To discern the boundaries of the PE more accurately, we utilized the c311-Gal4 driver, identified as a PE-specific Gal4 (Atkins & Mardon, 2009). Overlaying this signal, we observed that certain cells lacking typical PE morphology still exhibited the c311 signal (data not shown). Based on this observation, we noted that the PE is not composed entirely of perfect squamous cells but comprises subsections with diverse morphologies, encompassing cell types ranging from simple flat squamous cells to irregularly shaped cells. Consequently, we categorized the PE into 3-4 distinct types (Figure 8): central PE consisting of simple squamous cells, lateral PE comprising cuboidal cells, the intermediary zone (which is both part of PE and DP due to the lack of clear distinction) containing both cuboidal and columnar cells, and inner PE consisting of various cell types and structures.

Our findings underscore the pivotal role of the PE in the fusion process, as it emerges as the sole layer involved in the fusion of the pair of eye-antennal imaginal discs (Figure 7). The entire PE fusion process occurs during stage 3 and to a lesser extent in 4. At the beginning of stage 3, the inner PE of both discs can be distinguished, with only a small connection between them. This connection in the middle of stage 3 encompasses the entire inter-disc area and is facilitated by the zipping of the inner PE edges together. Once the connection is established, partial fusion of the PEs ensues, making it difficult to discern the left and right discs, resulting in the entire PE adopting an 'm' shape in transverse section (Figure 8).

The partial fusion progresses into complete fusion, achieved by an incision made in the epithelia separating the two lumens (Figure 7). This incision leads to the formation of a single continuous epithelium (or PE) covering the discs. During this process, some cells within the cut epithelium extrude out of the PE as round cells, while others migrate to adjacent regions of the PE. As a result, a substantial number of cells are lost from the entire complex, as we observed no cell division within the PE during this fusion process.

As we had some hint of the role of the inner PE, we wanted to understand the functions of the other PEs as well. Further examination revealed that the central PE serves as a temporary structure until stage 4, where no squamous cells are present (Figure 8). During stage 3, when dynamic PE movement mostly occurs, the central PE undergoes a transformation in cell shape. This process begins with an increase in cell area, followed by basal and apical constriction of the cell, along with lateral elongation, leading to a reduction in cell area. These cell reconstruction events occur at the whole tissue level within the central PE, resulting in a

reduction in the central PE area (Figure 8). The shrinking of central PE creates tension, causing the eyes to yield and be pulled from under the discs to the side.

During failed experiments, this tension hypothesis was indirectly verified. When an incision was made to the DP, the discs healed to some extent and did not significantly affect morphogenesis. However, any disruption or incision made to the PE resulted in the cessation of development most of the time. Similar findings were reported by Milner and colleagues (Milner et al., 1984), indicating that the PE provides tension. Our observations further suggest that a small area of the PE, the central PE, is responsible for providing motive force.

As the analysing of the lateral PE proved difficult, the roles of this PE subsection remain unknown to us.

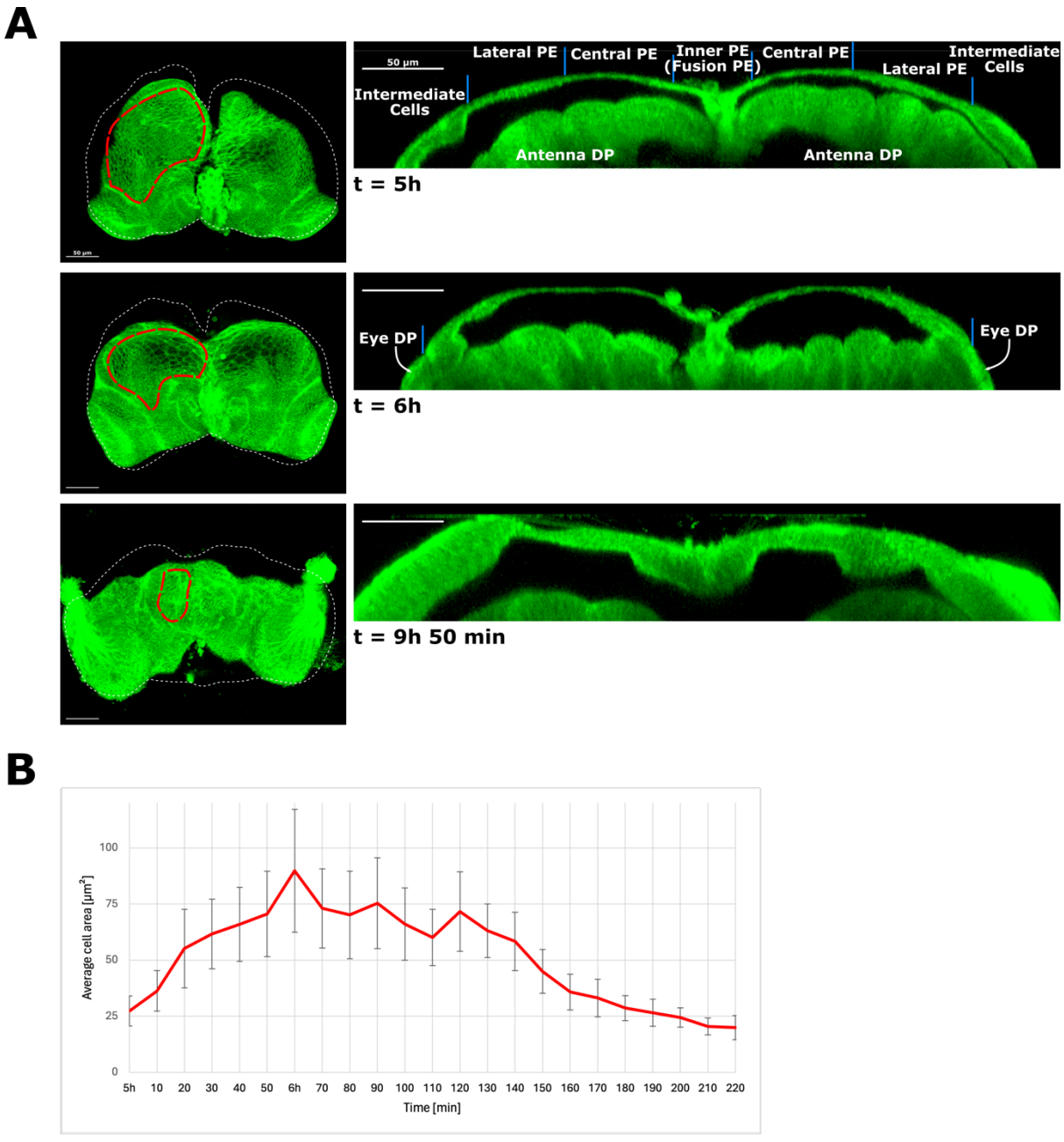

Figure 8. Eye-antennal imaginal disc tissue subsections and their role in the fusion process. (A) Time-lapse images of eye-antennal imaginal discs at 5 hours, 6 hours, and 9 hours 50 minutes after the start of culturing, showcasing the peripodial epithelium (PE). Left pictures show coronal sections, while the right shows transverse sections at corresponding times. The dashed white line in coronal sections delineates the whole head complex that was intentionally cropped to facilitate easier visualisation of the cell boundary within the PE. The dashed red line shows the area where typical squamous cells (central PE) are located. The right-most upper image (5h) shows variation of tissue types in the eye-antennal discs. Typical squamous cells are found within the central PE, while the lateral PE surrounds the central PE. Between the PE and disc proper (DP) is the intermediary zone, where cell types or PE and DP tissue boundaries cannot be distinguished. The inner PE shows the PE area responsible for fusion. (B) A graph with 95% confidence intervals that displays the change in the average cell area within the central PE (delineated by the red dashed line in (A)). Information regarding the definition of the central PE area and the creation of the graph can be found in section 2.2.5. Central PE cell area analysis. The observed shrinkage in cell area and movement of the eye DP in (A) suggests

that this tension provides the disc with the necessary force, like a pulley system, to induce drastic movements observed during ex vivo development. Scale bar: (A) 50 μm.

2.3.2.2. Mechanisms and Location of Fusion in Eye-Antennal Imaginal Discs

During the recent experiment with ubi-GFP-CAAX, we observed that during stage 3, adjacent epithelia exhibit a distinct thinner region. DIC imaging revealed that in the initial phase of stage 3, this region exhibits the presence of two distinct epithelia. Furthermore, this thinner area serves as an indication region of the incision site preceding fusion.

The above data have provided us with detailed single-cell resolution. However, it was challenging to determine the location of fusion and incision, and to comprehend the larger-scale morphogenetic changes. We proposed a hypothesis that the incisions and epithelial fusion of the two discs occur near the furrow, and cells in the tissue between the dorsal and ventral aspects extrude from the tissue. To test this hypothesis, we used DIC imaging to visualize the disc at the tissue level and CoinFLP (Figure 9) to randomly label a group of cells. This allowed us to track the movement of tissue in relation to the entire disc.

Utilizing DIC imaging combined with CoinFLP marking, we determined that fusion occurs within the discs, not near the furrow. As described, the incision precedes the fusion, and both occur near the same area. When an incision is made, the adjacent epithelia form initial fusion structures resembling a loop structure (Figure 9). Subsequently, this loop structure is slightly pulled apart and pushed outside by internal forces. Importantly, not all tissue separating the two lumens between the dorsal and ventral aspect is excised and removed. Tissue beneath the incision remains integral to the future head capsule composition, as evidenced by the outward displacement of tissue beneath the incision, as shown by CoinFLP cell group movement in (Figure 9). Moreover, thanks to the CoinFLP method randomly labelling cells, we identified the specific tissue area responsible for fusion, localized in the PE adjacent to the antennae during stage 1. This discovery lays the groundwork for further study of the underlying mechanisms involved during fusion.

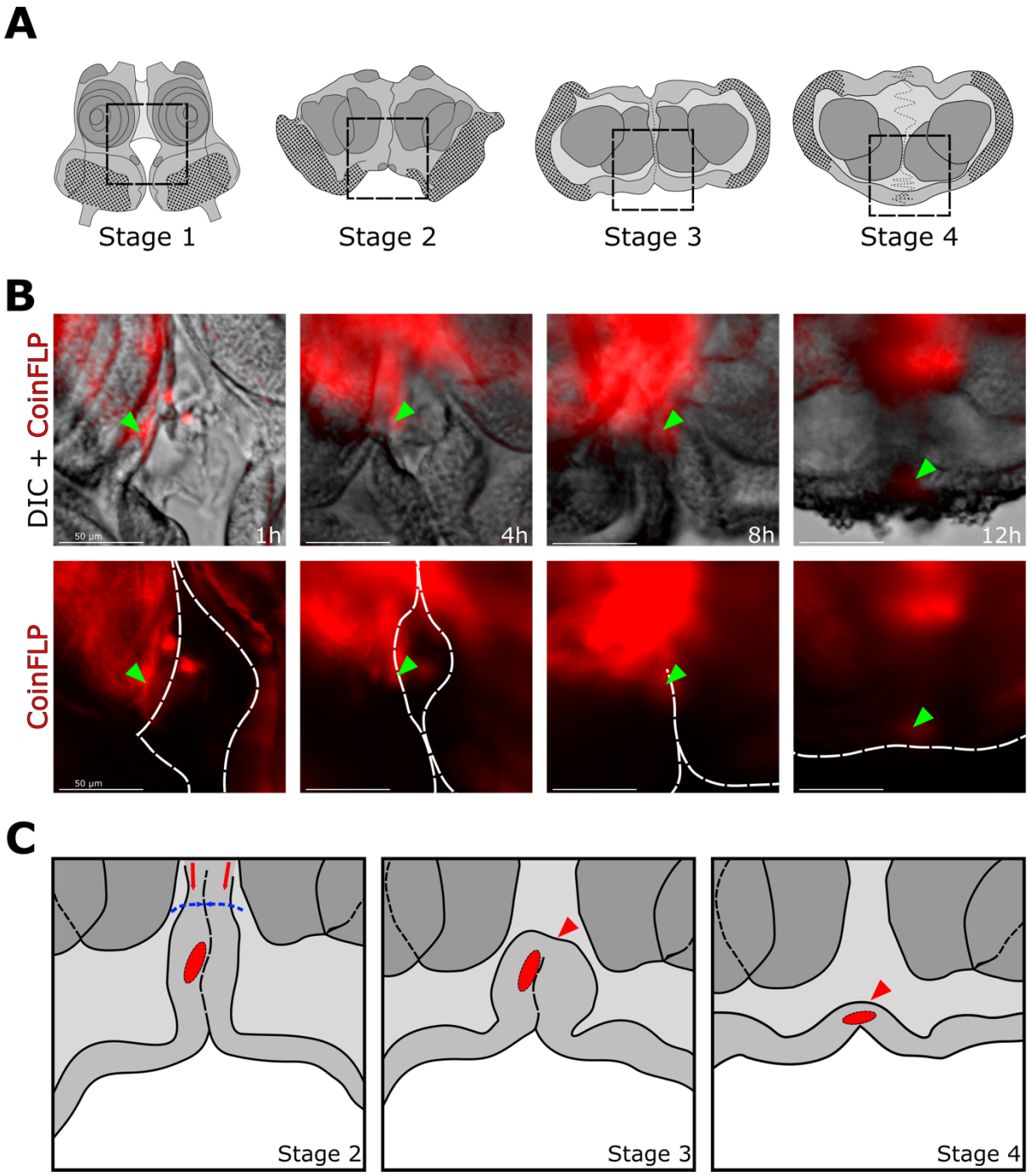

Figure 9. Location of the fusion area. (A) Locations of images (black square) represented in (B). (B) Fusion of two epithelia into a continuous layer. White dashed lines outline the tissue boundary. CoinFLP labelling was employed to randomly mark a group of cells, facilitating observation of their movement relative to the entire tissue. Notably, cells from the peripodial epithelium (PE) adjacent to the antennae will form the future dorsal aspect of the adult fly's head. The movement of the group of cells can be traced, indicated by green arrowheads. At the start of disc development, the pair are located in close proximity, with distinguishable left and right PEs. During stage 3 (between images captured at 4 and 8 hours), a swift incision is made to the epithelium, causing fusion of the two separate epithelia beneath the site. Subsequent developmental stages witness the gradual diminishment of the furrow formed during epithelial fusion, aided by internal forces exerted on the epithelia. (C) The movement of the group of cells and simplified representation of the fusion process. Red arrows mark the two distinct

epithelia, while blue dashed lines mark the location of the incision. The red arrowhead in both illustrations indicates the site of fused epithelia, previously situated underneath the incision area. Scale bar: (B) 50 μm.

2.3.3. Levels of Patterned Apoptosis are Elevated in a Band of PE Cells During Morphogenesis

Given the established importance of the PE in facilitating fusion during head morphogenesis, our research aimed to elucidate its underlying mechanism. Drawing from insights in other tissue fusion models (Hayes & Solon, 2017; H. Lu et al., 2015), we hypothesized that apoptosis might play a vital mechanical role throughout the developmental process. To investigate this, we initially employed CaspaseTracker (Figure 10) to detect whether the cells receive caspase-dependent apoptotic signals at specific times during development. It is worth noting that the CaspaseTracker biosensor detects cells with “recent” caspase activity, not in real-time. This is because the CaspaseTracker methodological approach leverages the sensitivity of the Gal4/UAS system, which tethers Gal4 to the cellular membrane where caspase activation typically occurs. Upon caspase 3 signal activation, Gal4 is released and transported to the nucleus (Figure 10). Consequently, downstream gene targets, including fluorescent proteins, are expressed some time later. This system inherently labels cells that are permitted to survive for at least a few hours, at least until the fluorescent protein is translated, since labelling depends on the Gal4/UAS system, that is driven by transcription, translation, and maturation of fluorescent protein. Only then can it be observed under the microscope. Thus, it is challenging to determine whether the signal indicates non-lethal, sub-lethal, or lethal apoptosis, only that the caspase 3 signal was received.

To explore the potential involvement of caspase signalling in eye-antennal imaginal discs, we employed a combination of CaspaseTracker with G-TRACE to detect both past and present activation of caspase 3 during *ex vivo* live imaging. Our observations revealed that cells with a "present" caspase 3 signal were specifically located at the fusion edges (Figure 10). The overlapping areas of the caspase 3 signal and fusion, along with a significant peak in signal strength at approximately 5 to 7 hours, corresponding to the stage 3 fusion time, suggest a potential role for caspase activity during the formation of the head.

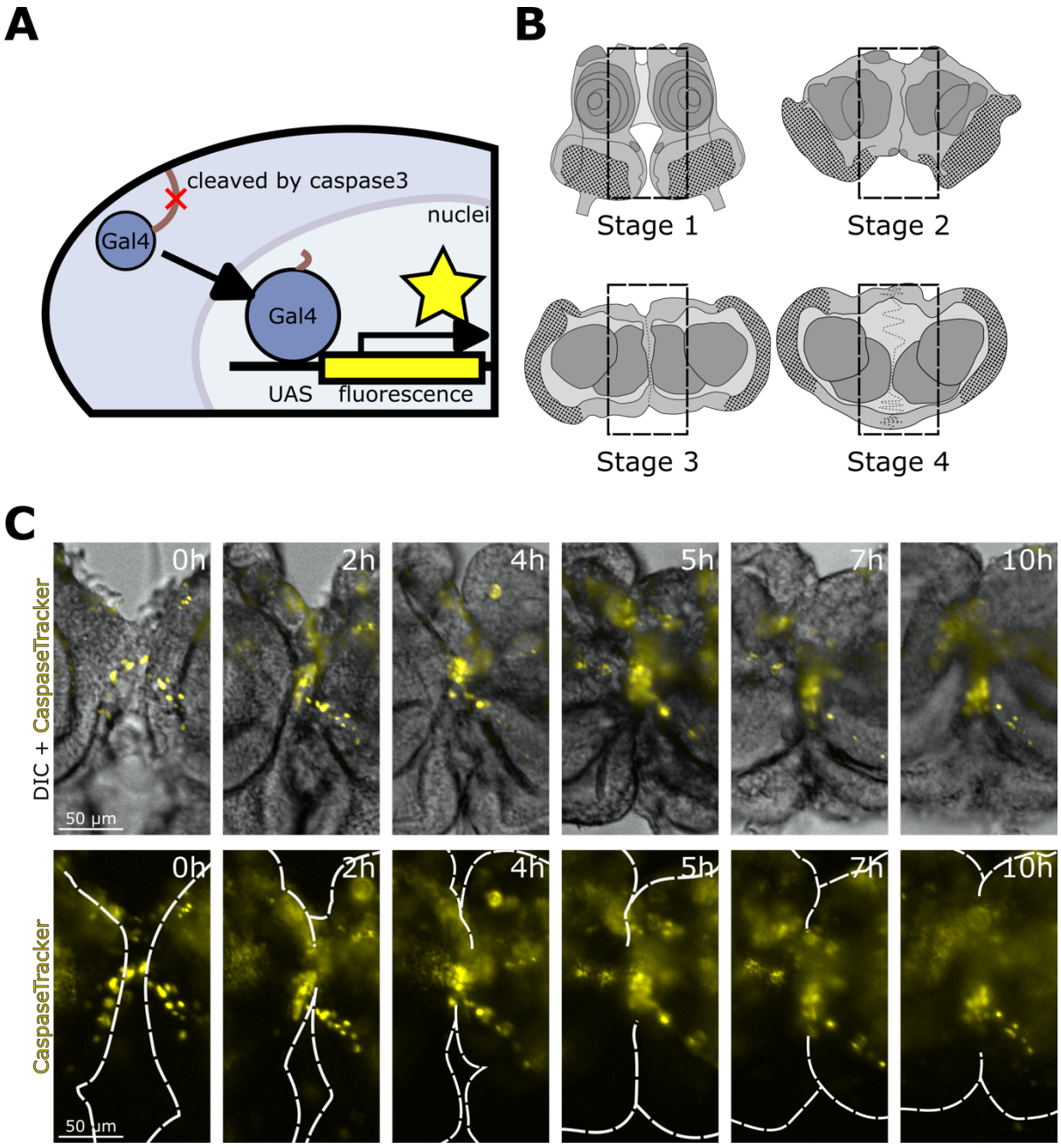

Figure 10. Patterning of apoptosis signal during development. (A) The CaspaseTracker was used to observe the dynamic signal of Caspase 3 during the fusion process. CaspaseTracker expresses a downstream gene target, allowing only the labelling of cells that survive for at least a few hours. Considering that typical apoptosis occurs within 1 hour in larval epidermal cells, this method may exhibit a bias towards cells that will not undergo apoptosis (Fujisawa et al., 2019). (B) Location of images depicted in (C). (C) DIC and CaspaseTracker expression (yellow) of the pair of eye-antennal discs at various time points. The dashed white line in CaspaseTracker only images indicate the location of the disc outline. CaspaseTracker expression is predominantly observed in the future fusion position, suggesting that Caspase 3 could be activated before epithelial fusion on each side. Scale bar: (C) 50 µm.

To validate the essential role of apoptosis, beyond just the caspase signal, during PE fusion, we explored additional genetic drivers to target the fusion area. This search led us to DE-Gal4

(Figure 11), which exhibits exclusive expression along the medial side of the discs, specifically within the PE. We crossed DE-Gal4 with UAS-p35, a cell death inhibitor, aiming to suppress apoptosis within the fusion area and observe resulting changes in adult flies, as *ex vivo* experiments were not successful for this purpose.

Due to DE-Gal4 being carried in a homozygous state with a balancer chromosome, this cross results in two distinct sets of progenies. One group carries the p35 apoptosis inhibitor and a balancer chromosome, thus showing no inhibition of apoptosis due to the utilization of the Gal4/UAS system and representing the "wild type" genotype. The other group carries the p35 apoptosis inhibitor and DE-Gal4, leading to flies with inhibited apoptosis only within the PE and between the discs.

Our findings revealed that only a handful of apoptosis inhibitor flies reached adulthood, with the pupal stage being particularly lethal. Among the surviving flies, 82% had a wild-type genotype, and 18% had an apoptosis inhibitor genotype. Ideally, following Mendelian principles, the progeny should be evenly distributed, with 50% representing the wild type and the other 50% representing the apoptosis inhibitor mutant genotype. However, the observed distribution indicates a significant difference in survival rates during fly development (Figure 11), emphasizing the necessity of apoptosis for healthy development.

Phenotypic analysis of the surviving adult flies revealed a spectrum of manifestations, ranging from no visible differences to severe abnormalities (Figure 11). Notably, the inhibition of apoptosis affected the right side of the head more frequently than the left side. The phenotypes were divided into four categories (Figure 11). Group 1 comprised flies with only head capsule-related phenotypes without any changes in the eyes. These head capsule-related phenotypes included scar tissue in the head capsule (similar to wrinkles, with some exhibiting black outgrowths on the epidermis), or a smaller or oblong head. Group 2 displayed minor eye phenotypes, such as a smaller round eye, heart-shaped eyes, or an oval-shaped eye that was sometimes also smaller than normal. Group 3 comprised flies that displayed severe eye phenotypes, such as a missing eye, or in rare cases, a mutation of the eye to an antenna. Lastly, Group 4 consisted of flies that had no change in phenotype.

Among the emerged apoptosis-inhibited adult flies, about half showed no change, while the other half displayed some form of head-related phenotype. Additionally, two-thirds of the flies with head-related issues displayed some form of eye-related phenotype. This underscores the

necessity of apoptosis during PE fusion of the eye-antennal imaginal discs to form a normal, functional head and head-related organs in the adult fly.

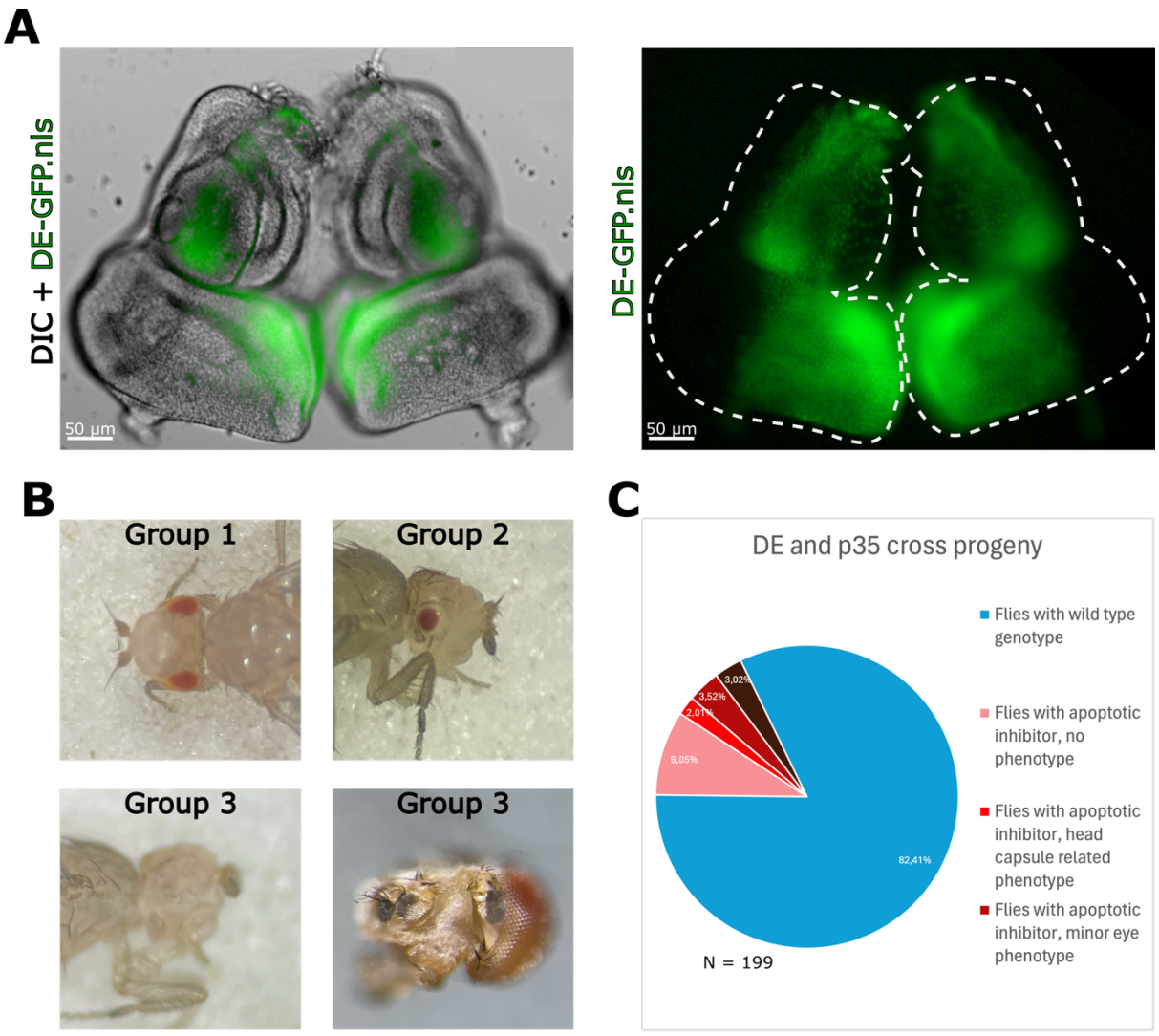

Figure 11. Effect of inhibiting apoptosis in the fusion area. (A) DIC and nuclear-localized DE-GFP expression of the pair of eye-antennal discs. With the focus on the peripodial epithelium (PE), the cell nuclei can be seen with no signal in the disc proper (DP), indicating the localisation of the signal only within the PE. Additionally, the signal localisation is only at the median side of the disc. (B) Different phenotypes observed when apoptosis was inhibited in the (A) location. This was done by crossing DE-Gal4 with p35, a cell death inhibitor obtained from the baculovirus p35. We classified the progeny of this cross into different groups. The upper-left image shows group 1, which exhibits head capsule-related phenotypes (such as an oblong or smaller head, or scar tissue near the eyes) without any changes in the eyes. In contrast, all flies in groups 2-3 showed varying degrees of change both in eyes and head capsule. The upper-right image shows group 2, displaying minor eye phenotypes (small round eyes, small/normal size oval eyes, or heart-shaped eyes). The lower two images show group 3, exhibiting severe eye phenotypes (either no eyes on the image on the left, or, in rare cases, eyes that have transformed into antennae, image on the right). (C) Graphs showcasing progeny statistics (all progeny N=199). Assuming Mendelian inheritance, the frequency of flies with wild type and apoptotic inhibitor mutants should be 50%. This illustrates that inhibition of apoptosis in the fusion PE region may be crucial for the metamorphosis of the fly. Out of the

flies with apoptosis inhibited (18%), about half (9%) showed some kind of head region-related phenotype different from the wild type of phenotype.

2.4. Discussion

Drosophila melanogaster imaginal discs have provided great insight into many aspects of development. Their growth and differentiation from simple epithelial sheets of a small number of cells to complex 3D organs consisting of thousands of cells help illuminate various biological events. The discs serve as a model for researching general developmental processes such as growth, proliferation, differentiation, morphogenesis, programmed cell death, and epithelial reorganization. In this bachelor's thesis, we introduce an *ex vivo* live imaging method that significantly extends the scope of imaginal discs as developmental models. The ability to track development in real time provides a potential tool for analysing most processes that occur in these discs.

Previous studies describing the metamorphosis of imaginal discs have primarily relied on observing dissected, fixed tissue or utilizing a single eye-antennal disc for *ex vivo* culturing (Tsao et al., 2016; Xu et al., 2021). This methodology presents challenges in understanding complex remodelling, lacks high-resolution continuity of events, introduces various fixation artifacts, and with single-disc studies, disallows the observation of development similar to that observed *in vivo*.

Comparing the wing discs and the eye-antennal discs, it can immediately be noticed how much less research has been done on the eye-antennal discs development, showcasing the problems with current methodologies for researching these discs. Still, our description of disc pair development aligns with previously reported data about developmental events like eyes rotation, inversion, and the PE providing motional force (Baker et al., 2014; Milner et al., 1983; Treisman & Heberlein, 1998). Combined with our complementary data from *ex vivo* studies, this allows us to state that our culture system is a more faithful reproduction of *in vivo* development than previous methods. Unsurprisingly, however, our protocol has revealed several previously unreported events. This again emphasizes the gap in *Drosophila* research and showcases the value of real-time direct observation of living tissue.

One of these previously undescribed morphogenetic events is the involvement of the PE in the fusion and subsequent composition of the adult head. The PE is widely believed to function only during larval development of all imaginal discs, after which it is removed. This belief

stems from observations in the most studied model, the wing disc (Tripathi & Irvine, 2022). With the eye-antennal discs, the DP is not the only layer contributing to the adult structure, and similar findings may be possible with other discs. Interestingly, when using ubi-GFP-CAAX to observe single cells and His2Av-RFP to mark chromosomes, no cell divisions were observed within the PE, making us wonder if the PE cells undergo mitosis later during fly metamorphosis or if the PE does not undergo any cell division.

The distinctive features of our developed culture methods include the capability to monitor disc development over extended periods (at least 20 hours) and the utilization of real-time 5D imaging under confocal microscopes for 3D tissue development reconstruction. This is an improvement in understanding *Drosophila ex vivo*, as previous methods allowed live imaging for 7 to 18 hours of a single disc (Tsao et al., 2016), but it is still not as good as some protocols allowing for 96 hours of culturing and observing pigmentation development (Gibbs & Truman, 1998; Milner et al., 1983, 1984). Another notable advantage is the technique's simplicity, as it does not require any observation chambers or reagents. Our live imaging of discs does not need any construction of specialized tools or reagents, such as the acquisition of large quantities of flies for fly extract, as we have found this unnecessary. This makes it more easily reproducible in various laboratories.

Although our data proved apoptosis to be an important key factor in disc pair fusion, we need to confirm in more detail the involvement of caspase signalling. As our experiment did not determine whether the caspase signalling is lethal or non-lethal, we still wonder if similar events occur where non-apoptotic caspase activation is involved in fusion, as it is in thorax closure and wound healing (Fujisawa et al., 2019). Alternatively, lethal caspase activation might be required to ensure that tissues and cell populations attain the appropriate size and correct alignment that allows fusion (Elmore, 2007; Noubissi et al., 2015).

In the future, our aim is to confirm the precise location of the initial connection and fusion. Based on our observations and suspicions, we hypothesize that the initial fusion will occur at the M zone cells. However, since these cells are difficult to distinguish, developing a more reliable method to localize different parts of the eye-antennal discs is necessary. More precise system could also further validate our other hypothesis that only the PE plays a major role in fusion and the formation of the head, while the DP is solely involved in the development of antennae and compound eyes.

Additionally, we are still working to confirm our findings, but we have identified three hot spots that need to meet each other to initiate fusion and form the correct head structure. One is near the maxillary palp, another near the ocelli region, and the last one on the median side of

the disc pair, close to the connection between the disc and mouthparts (Figure 12). We have gathered enough information about the maxillary hot spot to test whether inhibiting the connection is possible. Our findings indicate that when we use a wingless inhibitor, the regions near the maxillary palp consistently fail to meet and fuse, resulting in partial fusion of the discs and disconnected mouthparts area.

We aim to enhance our protocol for fusing eye-antennal imaginal discs from different organisms and species, with the objective of investigating the mechanisms and evolution of head morphogenesis from a different point of view. Thus far, we have already achieved success in imaging two independent eye-antennal discs from the same individual, with all the connections between the discs removed, to observe similar *ex vivo* development as demonstrated by our protocol. However, an experiment with less success involved imaging and fusing two independent eye-antennal imaginal discs from two different organisms, one emitting RFP and the other emitting GFP (Figure 12). While fusion has occurred only a handful of times and has been successful in showing development similar to our protocol, it needs further refinement and understanding. Should we succeed in refining this protocol, our next step will be to image and fuse discs from diverse fly species, such as *Drosophila silvestris*, a Hawaiian fly exhibiting sexual dimorphism in head development.

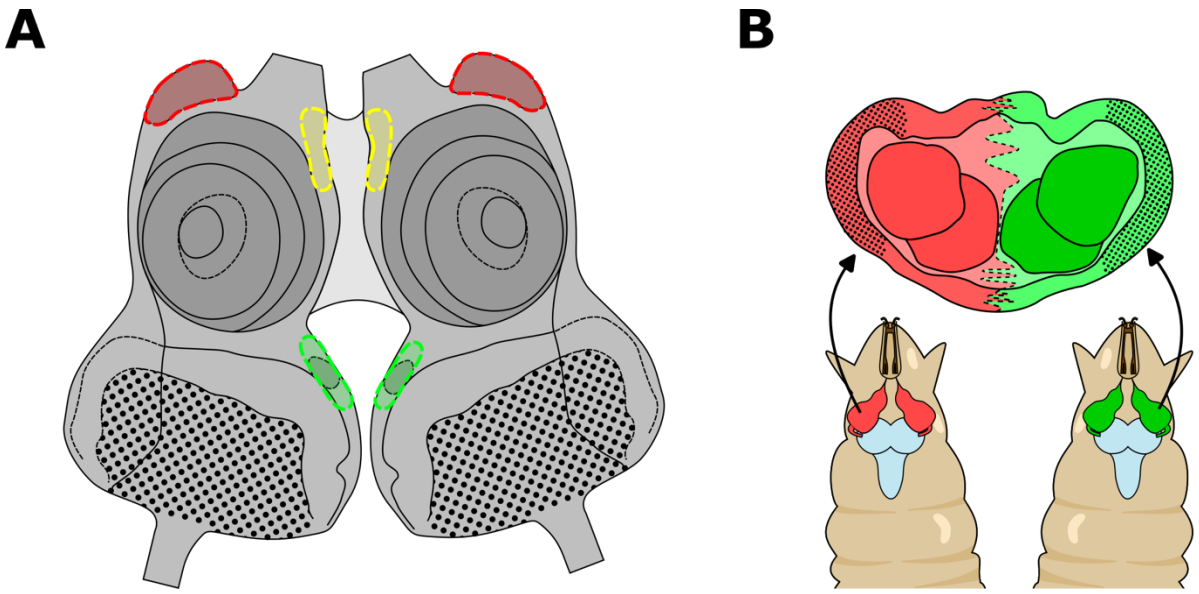

Figure 12. Future aims of this protocol. (A) Based on numerous *ex vivo* experiment observations, we propose that the fusion process involves three hot spots that need to interact to complete head formation. These three hot spots are located near the maxillary palps (red), between the pair near the connection to the mouthparts (yellow), and near the ocelli region (green). (B) In the future, as the protocol becomes more refined, we plan to fuse eye-antennal imaginal discs from different flies, such as one with a GFP genotype and another with an RFP

genotype. If this proves successful, we aim to expand the experiment by fusing discs from different *Drosophila* species.

Conclusion

In conclusion, our study presents a comprehensive analysis of the *ex vivo* culture method for observing head morphogenesis in *Drosophila* larval eye-antennal imaginal discs. Through systematic experimentation, we optimized the culture medium and dissection techniques to enable prolonged imaging sessions of the developing discs. By leveraging advanced microscopy technology, we captured dynamic morphogenetic events and coordinated fusion between the discs, uncovering previously unknown aspects of disc development. Our findings reveal four distinct stages of development, each characterized by specific morphological changes and events. These stages provide a framework for understanding the complex process of head morphogenesis from disc alignment to fusion and the formation of the definitive head cuticle. Furthermore, our comparison of *ex vivo* and *in vivo* development highlights the reliability of our *ex vivo* methods in reviewing key morphogenetic events observed *in vivo*. Additionally, we investigated the role of the peripodial epithelium (PE) in disc fusion and elucidated its dynamic involvement in the process. Our data suggest that the PE undergoes significant remodelling during development. We identified distinct subtypes of PE cells and demonstrated their specific contributions to fusion and tissue tension. Furthermore, our study implicates apoptosis as a crucial mechanism underlying PE fusion during head morphogenesis. By inhibiting apoptosis in the fusion area, we observed significant developmental abnormalities in adult flies, highlighting the essential role of apoptosis in ensuring normal head development. Overall, our research provides valuable insights into the mechanisms driving head morphogenesis in *Drosophila* and establishes a foundation for further studies on tissue fusion and organ development. The methodologies and findings presented here contribute to our understanding of developmental biology and may have implications for regenerative medicine and tissue engineering.

Äädikakärbse (*Drosophila melanogaster*) silma-tundla imaginaaldiskide *ex vivo* eluskoe reaalajas biokuvamine: kraniofatsiaalne morfogenees

Robin Sarv

Resümee

Kraniofatsiaalse - pea-näopiirkonna struktuuride kujunemine on keeruline arenguprotsess, mille käigus toimub mitmeid molekulaarseid ja morfogeneetilisi sündmusi. Äädikakärbse (*Drosophila melanogaster*) vastse peapiirkonna kujunemisel mängivad olulist rolli silma-tundla imaginaaldiskid. Morfogeneetilised sündmused ja mehhanismid, mis juhivad pea-näopiirkonna arengut, on paljuski ebaselged, kuna arengus toimuvaid dünaamilisi protsesse elusorganismides on keerukas uurida. Bakalaureusetöö üheks oluliseks eesmärgiks oli välja töötada täiustatud metoodika silma-tundla imaginaaldiskide uurimiseks *ex vivo* koekultuuri tingimustes, mis võimaldaks dokumenteerida pea-näopiirkonna kujunemist reaalajas, analüüsides ja selgitades olulisi arengulisi sündmusi morfogeneesi käigus.

Töö käigus optimeeriti süstemaatilise eksperimenteerimise tulemusel kultuurisöödet ja dissekteerimistehnikaid, et võimaldada imaginaaldiskide pikaajalist jälgimist ja biokuvamist. Lisaks arendati välja uudne *ex vivo* kultiveerimismeetod, mis võimaldas jälgida ja biokuvada kogu pea kujunemise protsessi reaalajas. Uurimuse käigus dokumenteeriti imaginaaldiskide dünaamilisi morfogeneetilisi protsesse, koordineeritud liikumisi ning imaginaaldiskide fuseerumist ehk liitumist, avastades seni teadmata aspekte peapiirkonna kujunemisel. Samal ajal näitasime esmakordselt dünaamilist arenguprotsessi, mille käigus silma-tundla imaginaaldiskide paari abil moodustub rudimentaarne sümmeetriline kärbse pea-näopiirkonna peastruktuur.

Töö tulemusena selgitati välja, et kärbse pea-näopiirkonna morfogeneesis ja imaginaaldiskide arengus toimub neli selgelt eristuvat arenguetappi, mis põhinevad spetsiifilistel morfoloogilistel muutustel ja arengusündmustel. Esimeses arenguetapis toimub imaginaaldiskide üksteisele lähemale tõmbumine ja kohakuti joondumine. Järgmises arenguetapis toimub kujuneva silma alge (silmadiski) ümberpööramine, mille käigus arenev silm muutub nõgusast kujust kumeraks. Kolmandas arenguetapis toimub silmadiskide liikumine, mille käigus alguses paralleelselt paikevad silmade alged pöörduvad eri suundadesse, moodustades 180-kraadise nurga nende vahele. Lisaks toimub selles etapis fuseerumise protsess. Neljandas arenguetapis jätkub fuseerumise sündmuste lõpuleviimine ja lõplik tervikliku peakapsli viimistlemine. Arengu alguses on kaks erinevat valendikku ehk

luumenit ja kaks imaginaaldiski, kuid lõpuks esineb vaid üks imaginaaldisk, mis ümbritseb üht luumenit.

Bakalaureusetöö oluliseks avastuseks oli peripodiaalse epiteeli (PE) dünaamiliste muutuste tuvastamine ning PE roll imaginaaldiskide fuseerumisel ja pea-näopiirkonna struktuuride moodustumisel. Varasemad teadustööd näitasid, et PE osaleb imaginaaldiskide arengus molekulaarsete signaalide allikana või ajutise struktuurina, mis aitab kaasa teatud arenguetapile. Meie uuringust selgus, et PE mitte ainult ei osale fuseerumises, vaid moodustab ka olulise osa pea-näopiirkonna struktuuridest edasises arengus. Lisaks oli märgatav ka apoptoosi roll pea-näopiirkonna struktuuride kujunemisel. Apoptoosi inhibeerimine äädikakärbeste vastse pea morfogeneesi kujunemisel võib põhjustada mitmesuguseid arenguhäireid, nagu näiteks silmade ja tundlate arenguhäired, kasvupeetus ning pea-näopiirkonna struktuuride ebaõige paiknemine.

Kokkuvõtteks on, et antud bakalaureusetöö tulemused olulised dünaamiliste ajaliselt-ruumiliselt kontrollitud arengumehhanismide mõistmiseks äädikakärbse pea-näopiirkonna struktuuride kujunemisel ja morfogeneesis. Samuti aitavad saadud tulemused arusaama luua keerukate epiteliaalsete struktuuride fuseerumise ja liitumise protsesside kohta. Bakalaureusetöö käigus väljatöötatud metoodikad omavad praktilist väärtust ning pakuvad head platvormi uute teadusküsimuste uurimiseks eluskudedes, mis võiksid olla abiks ka regeneratiivse meditsiini ja kudede tehnoloogia valdkonnas.

References

Aman, A., & Piotrowski, T. (2010). Cell migration during morphogenesis. *Developmental Biology*, *341*(1), 20–33. https://doi.org/10.1016/J.YDBIO.2009.11.014

Aranda, V., Nolan, M. E., & Muthuswamy, S. K. (2008). Par complex in cancer: A regulator of normal cell polarity joins the dark side. *Oncogene*, *27*(55), 6878. https://doi.org/10.1038/ONC.2008.340

Arranz, A., Dong, D., Zhu, S., Savakis, C., Tian, J., & Ripoll, J. (2014). In-vivo Optical Tomography of Small Scattering Specimens: time-lapse 3D imaging of the head eversion process in Drosophila melanogaster. *Scientific Reports*, *4*(1), 7325. https://doi.org/10.1038/srep07325

Atkins, M., & Mardon, G. (2009). Signaling in the third dimension: The peripodial epithelium in eye disc development. *Developmental Dynamics*, *238*(9), 2139–2148. https://doi.org/10.1002/dvdy.22034

Baker, N. E., Li, K., Quiquand, M., Ruggiero, R., & Wang, L. H. (2014). EYE DEVELOPMENT. *Methods (San Diego, Calif.)*, *68*(1), 252. https://doi.org/10.1016/J.YMETH.2014.04.007

Barone, V., & Heisenberg, C. P. (2012). Cell adhesion in embryo morphogenesis. *Current Opinion in Cell Biology*, *24*(1), 148–153. https://doi.org/10.1016/J.CEB.2011.11.006

Barwell, T., DeVeale, B., Poirier, L., Zheng, J., Seroude, F., & Seroude, L. (2017). Regulating the UAS/GAL4 system in adult Drosophila with Tet-off GAL80 transgenes. *PeerJ*, *5*, e4167. https://doi.org/10.7717/peerj.4167

Baum, B., & Georgiou, M. (2011). Dynamics of adherens junctions in epithelial establishment, maintenance, and remodeling. *The Journal of Cell Biology*, *192*(6), 907–917. https://doi.org/10.1083/JCB.201009141

Bosch, J. A., Tran, N. H., & Hariharan, I. K. (2015). CoinFLP: a system for efficient mosaic screening and for visualizing clonal boundaries in Drosophila. *Development*, *142*(3), 597–606. https://doi.org/10.1242/dev.114603

Brand, A. H., & Perrimon, N. (1993). Targeted gene expression as a means of altering cell fates and generating dominant phenotypes. *Development*, *118*(2), 401–415. https://doi.org/10.1242/dev.118.2.401

Bulgakova, N. A., & Knust, E. (2009). The Crumbs complex: from epithelial-cell polarity to retinal degeneration. *Journal of Cell Science*, *122*(15), 2587–2596. https://doi.org/10.1242/JCS.023648

Clarke, D. N., & Martin, A. C. (2021). Roles of the Actin Cytoskeleton and Cell Adhesion in Tissue Morphogenesis. *Current Biology : CB*, *31*(10), R667. https://doi.org/10.1016/J.CUB.2021.03.031

Cumming, J., & Wood, D. (2017). *Adult morphology and terminology [chapter 3]. In: Kirk-Spriggs, A.H. and Sinclair, B.J. (Eds.). Manual of Afrotropical Diptera: Volume 1, Suricata 4, SANBI Publications, Pretoria, pp. 89-133.* (pp. 89–133).

Eitzen, G. (2003). Actin remodeling to facilitate membrane fusion. *Biochimica et Biophysica Acta - Molecular Cell Research*, *1641*(2–3), 175–181. https://doi.org/10.1016/S0167-4889(03)00087-9

Elliott, A. D., Berndt, A., Houpert, M., Roy, S., Scott, R. L., Chow, C. C., Shroff, H., & White, B. H. (2021). Pupal behavior emerges from unstructured muscle activity in response to neuromodulation in Drosophila. *ELife*, *10*. https://doi.org/10.7554/eLife.68656

Elmore, S. (2007). Apoptosis: A Review of Programmed Cell Death. *Toxicologic Pathology*, *35*(4), 495. https://doi.org/10.1080/01926230701320337

Evans, C. J., Olson, J. M., Ngo, K. T., Kim, E., Lee, N. E., Kuoy, E., Patananan, A. N., Sitz, D., Tran, P., Do, M.-T., Yackle, K., Cespedes, A., Hartenstein, V., Call, G. B., & Banerjee, U. (2009). G-TRACE: rapid Gal4-based cell lineage analysis in Drosophila. *Nature Methods*, *6*(8), 603–605. https://doi.org/10.1038/nmeth.1356

Fagotto, F. (2015). Regulation of Cell Adhesion and Cell Sorting at Embryonic Boundaries. *Current Topics in Developmental Biology*, *112*, 19–64. https://doi.org/10.1016/BS.CTDB.2014.11.026

Fristrom, D. (1988). The cellular basis of epithelial morphogenesis. A review. *Tissue & Cell*, *20*(5), 645–690. https://doi.org/10.1016/0040-8166(88)90015-8

Fristrom, D., & Fristrom, J. W. (1993). The Metamorphic Development of the Adult Epidermis. In M. Bate & A. M. Arias (Eds.), *The Development of Drosophila melanogaster*. Cold Spring Harbor Laboratory Press.

Fujisawa, Y., Kosakamoto, H., Chihara, T., & Miura, M. (2019). Non-apoptotic function of Drosophila caspase activation in epithelial thorax closure and wound healing. *Development*, *146*(4). https://doi.org/10.1242/dev.169037

Germani, F., Bergantinos, C., & Johnston, L. A. (2018). Mosaic Analysis in Drosophila. *Genetics*, *208*(2), 473–490. https://doi.org/10.1534/genetics.117.300256

Gibbs, S. M., & Truman, J. W. (1998). Nitric oxide and cyclic GMP regulate retinal patterning in the optic lobe of Drosophila. *Neuron*, *20*(1), 83–93. https://doi.org/10.1016/S0896-6273(00)80436-5

Gibson, M. C., & Schubiger, G. (2000). Peripodial Cells Regulate Proliferation and Patterning of Drosophila Imaginal Discs. *Cell*, *103*(2), 343–350. https://doi.org/10.1016/S0092-8674(00)00125-2

Gillard, G., & Röper, K. (2020). Control of cell shape during epithelial morphogenesis: recent advances. *Current Opinion in Genetics & Development*, *63*, 1–8. https://doi.org/10.1016/J.GDE.2020.01.003

Girdler, G. C., & Röper, K. (2014). Controlling cell shape changes during salivary gland tube formation in Drosophila. *Seminars in Cell & Developmental Biology*, *31*, 74–81. https://doi.org/10.1016/J.SEMCDB.2014.03.020

Golic, K. G., & Lindquist, S. (1989). The FLP recombinase of yeast catalyzes site-specific recombination in the drosophila genome. *Cell*, *59*(3), 499–509. https://doi.org/10.1016/0092-8674(89)90033-0

Gumbiner, B. M. (1996). Cell Adhesion: The Molecular Basis of Tissue Architecture and Morphogenesis. *Cell*, *84*(3), 345–357. https://doi.org/10.1016/S0092-8674(00)81279-9

Hartenstein, V. (1993). *Atlas of Drosophila Development* (illustrated). Cold Spring Harbor Laboratory Press.

Hayes, P., & Solon, J. (2017). Drosophila dorsal closure: An orchestra of forces to zip shut the embryo. *Mechanisms of Development*, *144*, 2–10. https://doi.org/10.1016/J.MOD.2016.12.005

Haynie, J. L., & Bryant, P. J. (1986). Development of the eye-antenna imaginal disc and morphogenesis of the adult head in Drosophila melanogaster. *Journal of Experimental Zoology*, *237*(3), 293–308. https://doi.org/10.1002/jez.1402370302

He, L., Binari, R., Huang, J., Falo-Sanjuan, J., & Perrimon, N. (2019). In vivo study of gene expression with an enhanced dual-color fluorescent transcriptional timer. *ELife*, *8*. https://doi.org/10.7554/eLife.46181

Huttenlocher, A., & Horwitz, A. R. (2011). Integrins in Cell Migration. *Cold Spring Harbor Perspectives in Biology*, *3*(9), 1–16. https://doi.org/10.1101/CSHPERSPECT.A005074

Jacinto, A., Martinez-Arias, A., & Martin, P. (2001). Mechanisms of epithelial fusion and repair. *Nature Cell Biology 2001 3:5*, *3*(5), E117–E123. https://doi.org/10.1038/35074643

Jia, D., Jevitt, A., Huang, Y.-C., Ramos, B., & Deng, W.-M. (2022). Developmental regulation of epithelial cell cuboidal-to-squamous transition in Drosophila follicle cells. *Developmental Biology*, *491*, 113–125. https://doi.org/10.1016/j.ydbio.2022.09.001

Kalluri, R., & Weinberg, R. A. (2009). The basics of epithelial-mesenchymal transition. *The Journal of Clinical Investigation*, *119*(6), 1420. https://doi.org/10.1172/JCI39104

Keller, R. (2006). Mechanisms of elongation in embryogenesis. *Development*, *133*(12), 2291–2302. https://doi.org/10.1242/DEV.02406

Kenyon, K. L., Ranade, S. S., Curtiss, J., Mlodzik, M., & Pignoni, F. (2003). Coordinating Proliferation and Tissue Specification to Promote Regional Identity in the Drosophila Head. *Developmental Cell*, *5*(3), 403–414. https://doi.org/10.1016/S1534-5807(03)00243-0

Khalili, A. A., & Ahmad, M. R. (2015). A Review of Cell Adhesion Studies for Biomedical and Biological Applications. *International Journal of Molecular Sciences*, *16*(8), 18149. https://doi.org/10.3390/IJMS160818149

Kumar, J. P. (2018). The Fly Eye: Through the Looking Glass. *Developmental Dynamics : An Official Publication of the American Association of Anatomists*, *247*(1), 111. https://doi.org/10.1002/DVDY.24585

Kurn, H., & Daly, D. T. (2024, January). *Histology, Epithelial Cell*. StatPearls [Internet] Available from Https://Www.Ncbi.Nlm.Nih.Gov/Books/NBK559063/.

Lahr, E. C., Dean, D., & Ewer, J. (2012). Genetic Analysis of Ecdysis Behavior in Drosophila Reveals Partially Overlapping Functions of Two Unrelated Neuropeptides. *The Journal of Neuroscience*, *32*(20), 6819–6829. https://doi.org/10.1523/JNEUROSCI.5301-11.2012

Leggett, S. E., Hruska, A. M., Guo, M., & Wong, I. Y. (2021). The epithelial-mesenchymal transition and the cytoskeleton in bioengineered systems. *Cell Communication and Signaling : CCS*, *19*(1). https://doi.org/10.1186/S12964-021-00713-2

Lu, H., Sokolow, A., Kiehart, D. P., & Edwards, G. S. (2015). Remodeling Tissue Interfaces and the Thermodynamics of Zipping during Dorsal Closure in Drosophila. *Biophysical Journal*, *109*(11), 2406–2417. https://doi.org/10.1016/J.BPJ.2015.10.017

Lu, P., & Lu, Y. (2021). Born to Run? Diverse Modes of Epithelial Migration. *Frontiers in Cell and Developmental Biology*, *9*, 704939. https://doi.org/10.3389/FCELL.2021.704939/BIBTEX

Marchetti, M., Zhang, C., & Edgar, B. A. (2022). An improved organ explant culture method reveals stem cell lineage dynamics in the adult Drosophila intestine. *ELife*, *11*, 1–63. https://doi.org/10.7554/ELIFE.76010

Martin, A. C., & Goldstein, B. (2014). Apical constriction: themes and variations on a cellular mechanism driving morphogenesis. *Development (Cambridge, England)*, *141*(10), 1987. https://doi.org/10.1242/DEV.102228

McGuire, S. E., Le, P. T., Osborn, A. J., Matsumoto, K., & Davis, R. L. (2003). Spatiotemporal Rescue of Memory Dysfunction in Drosophila. *Science*, *302*(5651), 1765–1768. https://doi.org/10.1126/science.1089035

Mendonca, T., Jones, A. A., Pozo, J. M., Baxendale, S., Whitfield, T. T., & Frangi, A. F. (2021). Origami: Single-cell 3D shape dynamics oriented along the apico-basal axis of folding epithelia from fluorescence microscopy data. *PLOS Computational Biology*, *17*(11), e1009063. https://doi.org/10.1371/JOURNAL.PCBI.1009063

Milner, M. J., Bleasby, A. J., & Pyott, A. (1983). The Role of the Peripodial Membrane in the Morphogenesis of the Eye-Antennal Disc of Drosophila melanogaster. In *Arch Dev Biol* (Vol. 192).

Milner, M. J., Bleasby, A. J., & Pyott, A. (1984). Cell interactions during the fusion in vitro of Drosophila eye-antennal imaginal discs. In *Arch Dev Biol* (Vol. 193).

Milner, M. J., & Haynie, J. L. (1979). Roux's Archives of Developmental Biology Fusion of Drosophila Eye-Antennal Imaginal Discs During Differentiation in Vitro. In *Wilhelm Roux's Archives* (Vol. 185).

Mirzoyan, Z., Sollazzo, M., Allocca, M., Valenza, A. M., Grifoni, D., & Bellosta, P. (2019). Drosophila melanogaster: A Model Organism to Study Cancer. *Frontiers in Genetics*, *10*, 51. https://doi.org/10.3389/FGENE.2019.00051

Noubissi, F. K., Harkness, T., Alexander, C. M., & Ogle, B. M. (2015). Apoptosis-induced cancer cell fusion: a mechanism of breast cancer metastasis. *FASEB Journal : Official Publication of the Federation of American Societies for Experimental Biology*, *29*(9), 4036–4045. https://doi.org/10.1096/FJ.15-271098

Osterfield, M., Berg, C. A., & Shvartsman, S. Y. (2017). Epithelial Patterning, Morphogenesis, and Evolution: Drosophila Eggshell as a Model. *Developmental Cell*, *41*(4), 337–348. https://doi.org/10.1016/J.DEVCEL.2017.02.018

Osterwalder, T., Yoon, K. S., White, B. H., & Keshishian, H. (2001). A conditional tissue-specific transgene expression system using inducible GAL4. *Proceedings of the National Academy of Sciences*, *98*(22), 12596–12601. https://doi.org/10.1073/pnas.221303298

Pallavi, S. K., & Shashidhara, L. S. (2003). Egfr/Ras pathway mediates interactions between peripodial and disc proper cells in Drosophila wing discs. *Development*, *130*(20), 4931–4941. https://doi.org/10.1242/dev.00719

Pesch, Y. Y., Riedel, D., Patil, K. R., Loch, G., & Behr, M. (2016). Chitinases and Imaginal disc growth factors organize the extracellular matrix formation at barrier tissues in insects. *Scientific Reports*, *6*. https://doi.org/10.1038/SREP18340

Pignoni, F., & Zipursky, S. L. (1997). Induction of Drosophila eye development by Decapentaplegic. *Development*, *124*(2), 271–278. https://doi.org/10.1242/dev.124.2.271

Piroli, M. E., Blanchette, J. O., & Jabbarzadeh, E. (2019). Polarity as a physiological modulator of cell function. *Frontiers in Bioscience (Landmark Edition)*, *24*(3), 451. https://doi.org/10.2741/4728

Pollard, T. D., & Cooper, J. A. (2009). Actin, a Central Player in Cell Shape and Movement. *Science (New York, N.Y.)*, *326*(5957), 1208. https://doi.org/10.1126/SCIENCE.1175862

Rappel, W. J., & Edelstein-Keshet, L. (2017). Mechanisms of cell polarization. *Current Opinion in Systems Biology*, *3*, 43–53. https://doi.org/10.1016/j.coisb.2017.03.005

Riddiford, L. M., & Truman, J. W. (1993). Hormone Receptors and the Regulation of Insect Metamorphosis. *American Zoologist*, *33*(3), 340–347. http://www.jstor.org/stable/3883899

Rogers, B. T., & Kaufman, T. C. (1996). Structure of the insect head as revealed by the EN protein pattern in developing embryos. *Development*, *122*(11), 3419–3432. https://doi.org/10.1242/DEV.122.11.3419

Royet, J., & Finkelstein, R. (1995). Pattern formation in Drosophila head development: the role of the orthodenticle homeobox gene. *Development*, *121*(11), 3561–3572. https://doi.org/10.1242/dev.121.11.3561

Sakar, M. S., & Baker, B. M. (2018). Engineering Control over 3D Morphogenesis by Tissue Origami. *Developmental Cell*, *44*(2), 131–132. https://doi.org/10.1016/J.DEVCEL.2018.01.005

Scherzad, A., Hagen, R., & Hackenberg, S. (2019). Current Understanding of Nasal Epithelial Cell Mis-Differentiation. *Journal of Inflammation Research*, *Volume 12*, 309–317. https://doi.org/10.2147/JIR.S180853

Schneeberger, K., Roth, S., Nieuwenhuis, E. E. S., & Middendorp, S. (2018). Intestinal epithelial cell polarity defects in disease: lessons from microvillus inclusion disease. *Disease Models & Mechanisms*, *11*(2). https://doi.org/10.1242/dmm.031088

Schneider, I. (1964). Differentiation of larval drosophila eye-antennal Discs in Vitro. *Journal of Experimental Zoology*, *156*(1), 91–103. https://doi.org/10.1002/jez.1401560107

Schöck, F., & Perrimon, N. (2002). Molecular mechanisms of epithelial morphogenesis. *Annual Review of Cell and Developmental Biology*, *18*, 463–493. https://doi.org/10.1146/ANNUREV.CELLBIO.18.022602.131838

Suzuki, M., Morita, H., & Ueno, N. (2012). Molecular mechanisms of cell shape changes that contribute to vertebrate neural tube closure. *Development, Growth & Differentiation*, *54*(3), 266–276. https://doi.org/10.1111/J.1440-169X.2012.01346.X

Svitkina, T. (2018). The Actin Cytoskeleton and Actin-Based Motility. *Cold Spring Harbor Perspectives in Biology*, *10*(1). https://doi.org/10.1101/CSHPERSPECT.A018267

Tanguay, R. M., & Morrow, G. (2008). Neural Expression Of Small Heat Shock Proteins Influences Longevity And Resistance To Oxidative Stress. In *Heat Shock Proteins and the Brain: Implications for Neurodegenerative Diseases and Neuroprotection* (pp. 319–336). Springer Netherlands. https://doi.org/10.1007/978-1-4020-8231-3_16

Tepass, U., Tanentzapf, G., Ward, R., & Fehon, R. (2001). Epithelial Cell Polarity and Cell Junctions in Drosophila. *Annual Review of Genetics*, *35*(1), 747–784. https://doi.org/10.1146/annurev.genet.35.102401.091415

Todi, S. V., Sharma, Y., & Eberl, D. F. (2004). Anatomical and molecular design of the Drosophila antenna as a flagellar auditory organ. *Microscopy Research and Technique*, *63*(6), 388–399. https://doi.org/10.1002/jemt.20053

Treisman, J. E., & Heberlein, U. (1998). 4 Eye Development in Drosophila: Formation of the Eye Field and Control of Differentiation. *Current Topics in Developmental Biology*, *39*, 119–158. https://doi.org/10.1016/S0070-2153(08)60454-8

Tripathi, B. K., & Irvine, K. D. (2022). The wing imaginal disc. *Genetics*, *220*(4). https://doi.org/10.1093/GENETICS/IYAC020

Tsao, C. K., Ku, H. Y., Lee, Y. M., Huang, Y. F., & Sun, Y. H. (2016). Long Term Ex Vivo Culture and Live Imaging of Drosophila Larval Imaginal Discs. *PLoS ONE*, *11*(9). https://doi.org/10.1371/JOURNAL.PONE.0163744

Walck-Shannon, E., & Hardin, J. (2014). Cell intercalation from top to bottom. *Nature Reviews Molecular Cell Biology*, *15*(1), 34–48. https://doi.org/10.1038/nrm3723

Weasner, B. M., Zhu, J., & Kumar, J. P. (2017). *FLPing Genes On and Off in Drosophila* (pp. 195–209). https://doi.org/10.1007/978-1-4939-7169-5_13

Weasner, B. P., & Kumar, J. P. (2022). The early history of the eye-antennal disc of Drosophila melanogaster. *Genetics*, *221*(1). https://doi.org/10.1093/genetics/iyac041

Xu, Y., Shrestha, N., Préat, V., & Beloqui, A. (2021). An overview of in vitro, ex vivo and in vivo models for studying the transport of drugs across intestinal barriers. *Advanced Drug Delivery Reviews*, *175*, 113795. https://doi.org/10.1016/J.ADDR.2021.05.005

Younossi-Hartenstein, A., Tepass, U., & Hartenstein, V. (1993). Embryonic origin of the imaginal discs of the head of Drosophila melanogaster. *Roux's Archives of Developmental Biology*, *203*(1–2), 60–73. https://doi.org/10.1007/BF00539891

Yu, H.-H., Chen, C.-H., Shi, L., Huang, Y., & Lee, T. (2009). Twin-spot MARCM to reveal the developmental origin and identity of neurons. *Nature Neuroscience*, *12*(7), 947–953. https://doi.org/10.1038/nn.2345

Yu, W., & Hill, W. G. (2011). Defining protein expression in the urothelium: a problem of more than transitional interest. *American Journal of Physiology-Renal Physiology*, *301*(5), F932–F942. https://doi.org/10.1152/ajprenal.00334.2011

Zartman, J. J., & Shvartsman, S. Y. (2010). Unit operations of tissue development: Epithelial folding. *Annual Review of Chemical and Biomolecular Engineering*, *1*(Volume 1, 2010), 231–246. https://doi.org/10.1146/ANNUREV-CHEMBIOENG-073009-100919/CITE/REFWORKS

Non-exclusive licence to reproduce the thesis and make the thesis public

I, Robin Sarv,

1. grant the University of Tartu a free permit (non-exclusive licence) to reproduce, for the purpose of preservation, including for adding to the DSpace digital archives until the expiry of the term of copyright, my thesis

   "Live Imaging of Drosophila melanogaster Eye-Antennal Imaginal Disc Ex vivo Culture: Craniofacial Morphogenesis"

   supervised by Vi Ngan Tran and Osamu Shimmi

2. I grant the University of Tartu a permit to make the thesis specified in point 1 available to the public via the web environment of the University of Tartu, including via the DSpace digital archives, under the Creative Commons licence CC BY NC ND 4.0, which allows, by giving appropriate credit to the author, to reproduce, distribute the work and communicate it to the public, and prohibits the creation of derivative works and any commercial use of the work until the expiry of the term of copyright.

3. I am aware of the fact that the author retains the rights specified in points 1 and 2.

4. I confirm that granting the non-exclusive licence does not infringe other persons' intellectual property rights or rights arising from the personal data protection legislation.

Robin Sarv
27/05/2024